Master's Thesis

Master's Degree in Energy Engineering

Development of a model to simulate solar PV plants in MATLAB with a study on the effects of under-sizing the inverter

Master's Thesis

Gabriele Catalano
Oriol Gomis Bellmunt
September 2018

Escola Tècnica Superior
d'Enginyeria Industrial de Barcelona

Abstract

The solar PV market is continuously expanding and utility-scale solar plants are becoming larger due to advantages in economies of scale. Consequently, it is an increasingly important part of the design to have reliable simulation software allowing investors and engineers to make financial and technical decisions. Moreover, for expert users it is important to have a flexible software in which every model can be tuned and adjusted. To address this issue, the present thesis proposes the development of a MATLAB based program to simulate hourly production of solar PV systems. It includes an application of the software in which the economic feasibility of under-sizing the inverter is studied. To create the model, all the equations are taken from either PVsyst or SAM and the algorithms used are explained in details. In the analysis on under-sizing the inverter, a 10 MW PV plant is designed and the LCOE as a function of the DC-to-AC ratio is analyzed for different locations. Results of the program against the reference software show that the hourly RMSE for the DC power is 0.26%. The analysis showed that an optimal DC-to-AC ratio for which LCOE is minimum can be found. The reduction in total LCOE and total capex is respectively around 3.3-3.7% and 4% depending on the location. Conclusions are that a flexible open source MATLAB code could be developed with high accuracy and that under-sizing the inverter make economic sense if carefully performed.

Table of contents

Tables and figures

Figures

Tables

List of abbreviations

LCOE=levelized cost of electricity

WACC=weighted average cost of capital

CAPEX=capital expenditure

OPEX=operating expense

RES=renewable energy source

IRR=internal rate of return

IRENA=international renewable energy agency

IEA=international energy agency

GHI=global horizontal irradiance

DHI=diffuse horizontal irradiance

BHI=beam horizontal irradiance

DNI=direct normal irradiance

POA=plane of array

DC= direct current

AC=alternate current

MPPT=maximum power point tracking

G=irradiance (W/m2)

CF=Capacity Factor

PV=photovoltaics

1. Introduction

1.1. Objective

This work focuses on the development of a model to simulate the production of solar photovoltaic (PV) plants in MATLAB. The model starts from the value of global horizontal irradiation (GHI) and calculates all the necessary quantities needed to predict the production with hourly time steps. It is included in this project an application of the model to perform a study on the effects of under-sizing the inverter on the project's capital expenditure (CAPEX) and levelized cost of electricity (LCOE).

1.2. Motivation

The purpose of this project is to develop a MATLAB based program to simulate PV plants and leave the code to the research center CITCEA at the Polytechnic University of Catalonia (UPC) where it was developed. The idea is that this program may be extended by other students and could help from both a didactic and a research viewpoint.

Among the different renewable technologies, this project focuses on solar PV plants because I personally believe that solar PV has an enormous potential to become a fundamental player in the future energy mix. It will have a great impact in mitigating climate change, and it can help many of the developing countries to go out form energy poverty and obtain access to economic and clean energy. Although this motivation is personal, it is backed by numbers and recent trends presented in the section 1.4 on the overview on solar PV energy.

1.3. Scope

The scope of the present project is limited to the study and implementation in MATLAB of models to simulate the behavior of the different steps needed to convert the solar irradiance to electricity. This process is divided and studied to a level of degree similar to the software PVsyst that has been used as the reference. Obviously, PVsyst has a much larger scope and includes many different models to simulate a great variety of situations (such as the 3-D shade study etc.). Instead, the scope of this project is limited to the simulation of grid connected PV plant, with multi or mono crystalline silicone modules and considering in details only the energy conversion from irradiance to the output of the DC-AC inverters, without considering the integration to the grid. A detailed list of the models included in this project is included in section 4.2. For each model that describes a physical phenomenon, the focus is on finding the best way to model the phenomenon in a simulation program and not on the theory of the physical phenomenon itself. The detailed methodology followed while developing the model can be found in section 4.1. Moreover, this project focuses on the application of PV technologies and not on the technology itself, therefore the different kinds of PV technologies are not analyzed and in the development of the model, it is always

assumed that the silicon technology is used (both mono and multi-crystalline) because it is the technology most spread in the market [1].

Finally, the present program was built from scratch so that the scope had to be limited with a trade-off between results and resources. Nevertheless, the software developed could be extended by others with several interesting further works, which is one of the aim of the project and is discussed in details in Section **¡Error! No se encuentra el origen de la referencia.**.

1.4. Structure

The project is structured in different sections. After this introduction, Section 2 introduces a general view on the photovoltaic sector, its crucial importance for a shift to a cleaner energy supply and its tremendous potential with a focus on the recent trends in LCOE and CAPEX for solar PV plants. Section 3 introduces a short review on the fundamental concepts of irradiance in outer space and on the Earth's surface needed as the basis for what follows. Section 4 describes the model developed in this project: every sub-model is described and all the equations, algorithms and assumptions used in the model are explained in details. Section 5 presents a validation of the model against the commercial software PVsyst and SAM. Section 6 deals with the study of the effects of under-sizing the inverter on the CAPEX and LCOE of a solar PV plant. The analysis is performed using weather data from different locations and equal plant design. Section 7 introduce the environmental Impact and the financials of developing a solar PV plant. In Section 8, the conclusions of the project are presented, with a view on possible further studies.

2. A general view on the photovoltaic market

PV systems play an important role in the energy mix of several countries. In Germany, Italy and Greece for instance, the energy generated in 2015 by PV systems accounted respectively for more than 7% of the electricity need and in Europe the average was almost 4% in 2015 [2].From a global perspective, the PV market experienced a rocket growth in the last years: the global PV installed capacity grew from 6.1GW in 2010 to 291GW in 2016, which means 47 times larger, which is clearly visible in the figure below from [1]:

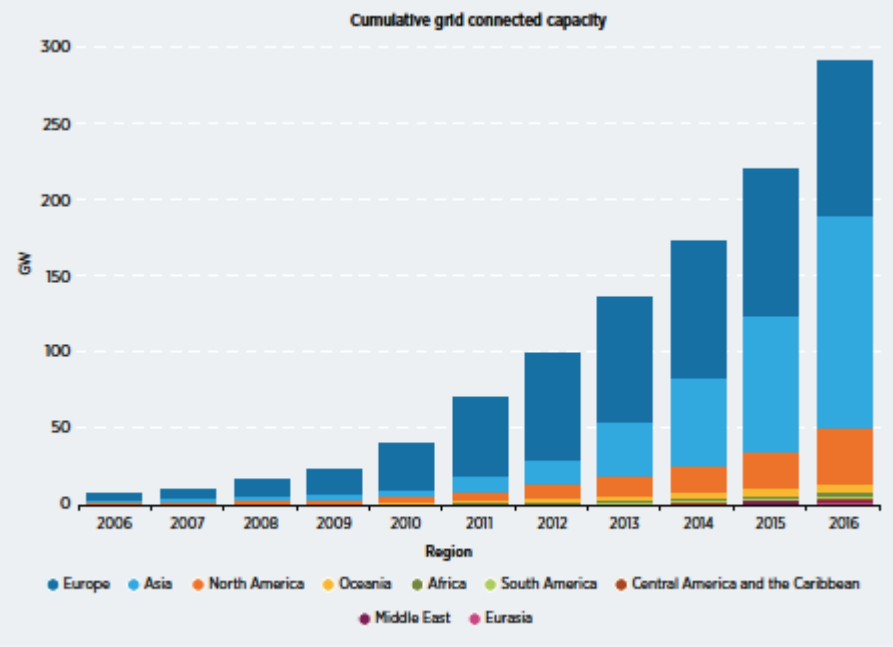

Source: IRENA, 2017a.

Figure 1: Commutative grid connected capacity in the years from 2006 to 2016 divided by macro-regions. Source IRENA [1]

The reasons for such a rapid growth of the PV market can be traced back to two main drivers. Firstly, the policies for reduction of greenhouse gases emissions play a fundamental role and are now present in the most of the countries, for example Europe set a target of 20% reduction of CO2 emissions by 2020 [3]. A clear example that shows the great impact of policies in the growth of installed capacity is the situation the happened in Italy. There, thanks to subsidies and policy for a profitable Feed-in Tariff, the PV market of the country grew rapidly during the years of the policy that was available between 2005-2013. When the strong financial incentives were not available anymore, annual installed capacity additions remained stable or even fell: added capacity in 2015 was 300MW while in 2014 it was 424MW. Nevertheless, the electricity generated by PV in the country remains remarkably high, with 8.2% of the energy needs coming from PV in 2016 [2].

The second main reason is the reduction of LCOE of PV systems which makes it appealing for new

investors: this is actually both a driver and an effect because expansion driven by lower prices brings economy of scales which further reduces the costs [4]. The LCOE is good indicator to compare different technologies because it is independent of the specific technology as it represents the all the costs of producing one unit of energy (Kwh, Mwh etc.) with a particular technology considering the whole lifetime of the project. It can also be thought of as the minimum costs at which energy should be sold to reach specific return on investment (for details on the formula of LCOE and the models used in this work see section 4.12). For these reasons, the following section is dedicated to a brief overview of the LCOE in PV systems.

2.1. LCOE of PV systems

To have an idea of the trends of LCOE, the following graph compares the LCOE of the different renewable energy sources (RES), with global averages from 2010 to 2017 elaborated by IRENA [1]:

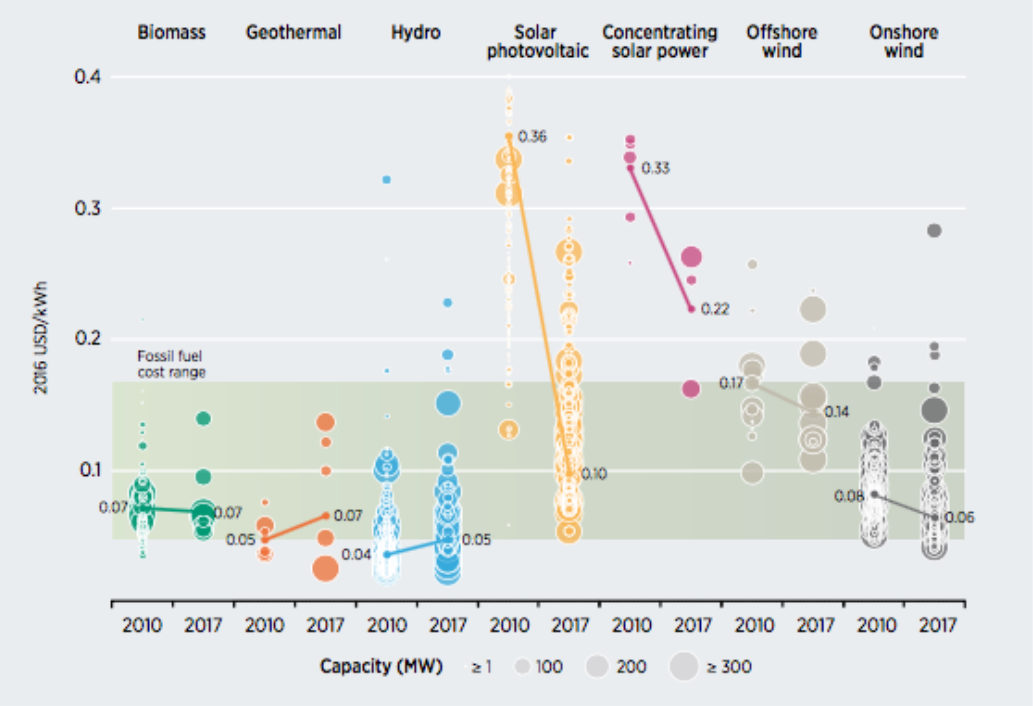

Source: IRENA Renewable Cost Database.

Figure 2 Levelized cost of electricity (LCOE) for different renewable energy technologies in 2010 and 2017 from global averages. Source IRENA [1].

The LCOE of solar photovoltaics has experienced a rapid drop of 72.2% in only 7 years, with values around 0.36USD/KWh (or 360 USD/MWh) in 2010 compared to 0.1 USD/KWh (or 100 USD/MWh) in 2017. In this case IRENA used weighted average cost of capital (WACC) of 7.5% for OECD countries and china while 10% for the rest of the world (for a detailed description of WACC see Section 4.12). It is interesting to see how the LCOE of PV projects is already in the fossil fuel LCOE

range, which means that the technology without subsidies is already cost competitive if compared with conventional fossil fuel power generation. As a consequence, PV systems already reached the grid parity in many countries [1].

The main driver for this rapid drop in the LCOE is clearly the reduction in CAPEX that decreases the investment needed to build a plant and the increase in capacity factor which increases the amount of energy produced given the same plant. The figure below from IRENA [1] clearly shows these trends:

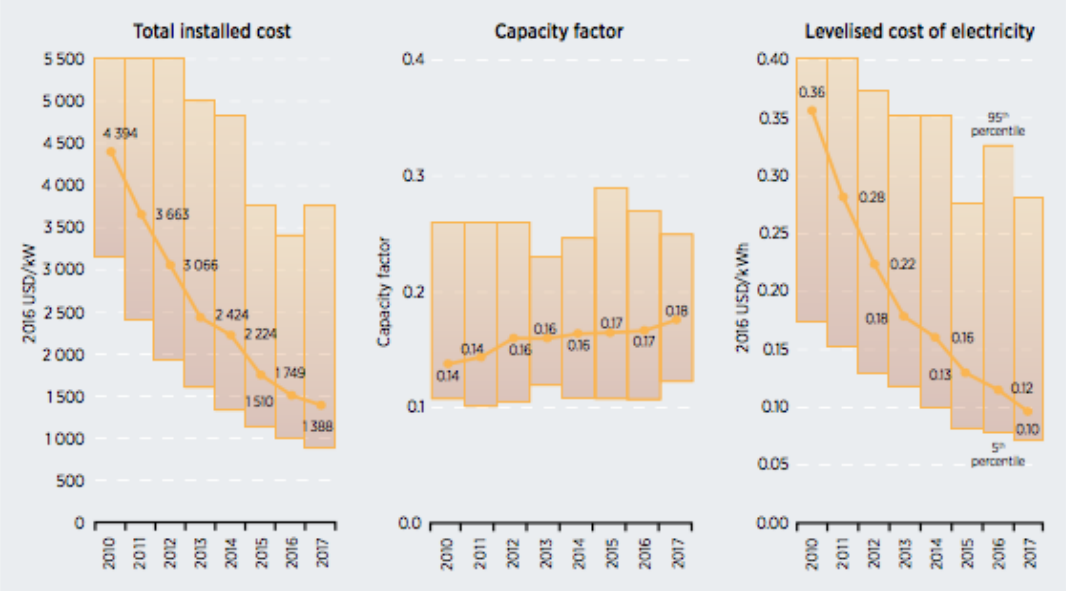

Source: IRENA Renewable Cost Database.

Figure 3 Total installed cost, capacity factor and levelized cost of electricity (LCOE) for solar PV plants in the years from 2010 to 2017 (global averages). Source IRENA [1].

The installed cost fell from 4394 USD/kW in 2010 to 1388 USD/kW in 2017, while the capacity factor grew from 0.14 to 0.18 in the same years, meaning that given the same amount of installed power, a PV plant in 2017 generated on average 28.6% more than a plant in 2010. As a consequence of these two factors, the LCOE on the right fell from 0.36USD/kWh to 0.10 USD/kWh from 2010 to 2017.

The numbers above are global averages, with projects from all around the world, but clearly the LCOE of a PV plant is very much related to its position and to the irradiance of the particular location: with a higher average irradiance, the LCOE is expected to be lower. As an example, the chart below shows the forecasted trend in LCOE (with real data from 2016) for a 1MW PV plant in Madrid for different values of WACC [5]:

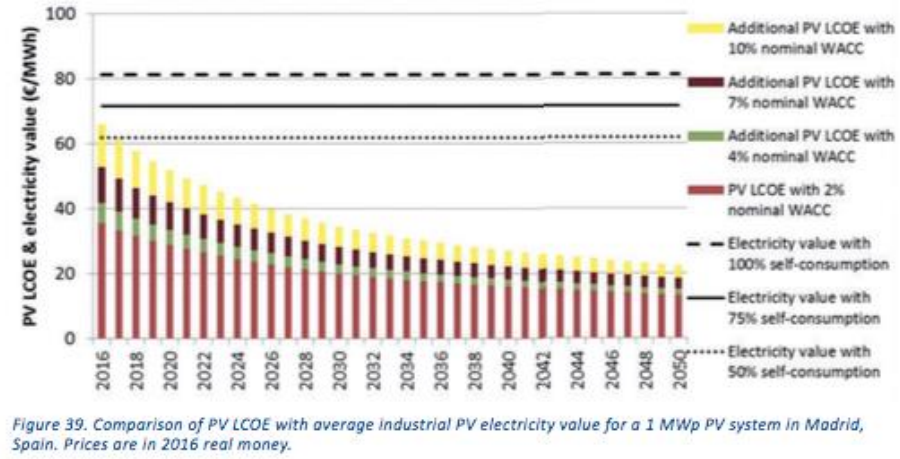

Figure 4 Comparison of levelized cost of electricity (LCOE) with electricity value for a 1 MW PV system in Madrid from 2016 to 2050. LCOE is calculated with different WACC. Source [5].

Different colors in the chart represent different values for WACC. As it can be seen, already in 2016 the LCOE for a plant in Madrid even with a WACC of 10%, is lower than 70 eur/MWh (0.7 eur/kWh), which is the electricity value with 75% of self-consumption and obviously it is even lower with a lower WACC.

Similarly, the chart below shows the LCOE for a 50 MW PV plant in Rome:

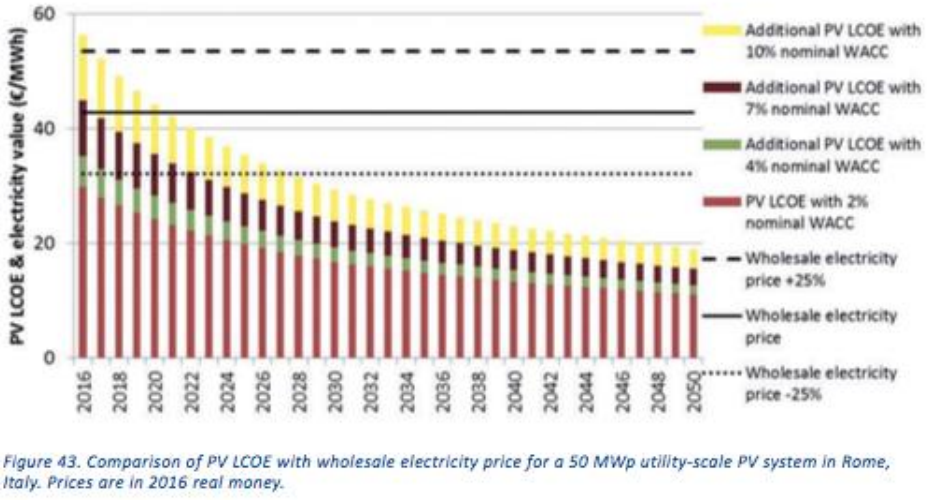

Figure 5 Comparison of LCOE with wholesale electricity price for a 50MW PV system in Rome, Italy from 2016 to 2050. Source [5].

Here the lines represent wholesale electricity price. With a WACC of 7% the LCOE is around 40 eur/MWh (0.4 eur/kWh), which is already under the average wholesale electricity price, making the technology cost competitive and making it reach the grid parity.

3. Review of basic concepts for the modeling of PV

In this section, the concepts of extraterrestrial irradiance and the different components of the irradiance on the Earth's surface are briefly introduced. These quantities are needed for the calculation of the Erb's equation and the plane of array (POA) irradiance explained respectively in sections 4.3.2 and 4.5.

3.1. Extraterrestrial Irradiance

The solar irradiance outside the atmosphere of the Earth is a function of the distance Sun-Earth. Since the distance is almost constant over the year with a mean value of 1.495 $\times 10^{11}$ m the irradiance in outer space is almost constant and the flux at the mean distance can be defined. This quantity, called "solar constant", is equal to 1361 W/m^2 and is defined as the flux received on a surface normal to the direction of the beam and calculated at a mean Earth-Sun distance [6]. However, for the development of this project a more precise value of the extraterrestrial irradiance is needed considering that the distance Earth-Sun varies slightly throughout the year, leading the actual extraterrestrial irradiance to vary depending on the day of the year according to:

$$I_0 = G_{sc} \times (1.000110 + 0.034221 \cos B + 0.001280 \sin B + 0.000719 \cos 2B + 0.000077 \sin 2B) \quad (3.1)$$

Where G_{sc} is the solar constant and the year angle B is defined as:

$$B = \frac{n-1}{365} 2\pi \quad (3.2)$$

In addition, it is necessary to calculate the extraterrestrial irradiance horizontal to the Earth's surface, needed to calculate the clearness index K_t which is fundamental in Erb's correlation (see Section 4.3.2).The extraterrestrial horizontal irradiance is given by:

$$I_{0h} = I_0 \cos \theta_z \quad (3.3)$$

And the clearness index, can be defined as:

$$K_t = \frac{GHI}{I_{0h}} \quad (3.4)$$

Where GHI is the global horizontal irradiance in W/m2 (explained in the following section) and θ_z is the zenith of the Sun in radians(calculated in Section 4.4.3.3).

Similarly, the clearness index of the beam, used in the calculation of sky-diffuse calculation (see

section 4.5.5) can be calculated as:

$$K_b = \frac{BHI}{I_{0h}} = \frac{DNI}{I_0} \tag{3.5}$$

Where BHI and DNI are respectively the beam horizontal irradiance and the direct normal irradiance explained in the following section.

3.2. The different components of the irradiance

In this section the concepts of global, diffuse, beam and direct normal irradiance are presented. The extraterrestrial irradiance described in section 3.1 passes through the atmosphere before reaching the Earth's surface. During its journey, a part of it is absorbed, reflected, and diffracted by the atmosphere. Therefore the irradiance reaching the surface of a module is lower and can be seen as divided in two parts: a beam component, aligned with the direction of the sun beams, and a diffuse component, coming from the reflection and diffraction of the atmosphere and the reflection of the Earth's surface (called albedo). Together they form the global irradiance. Since the irradiance is a flux, it is important to define the orientation of the surface to which it is referred. Generally, the irradiance is typically measured on a horizontal surface: global horizontal irradiance (GHI), diffuse horizontal irradiance (DHI), and beam horizontal irradiance (BHI) are the three components referred to a horizontal surface and are related by:

$$GHI = BHI + DHI \tag{3.6}$$

Where BHI is the projection of the direct normal irradiance (DNI) on a horizontal surface:

$$BHI = DNI \cos\theta_z \tag{3.7}$$

DNI is the direct normal irradiance, which is the beam irradiance referred to a surface normal to the direction of the sun. The zenith of the Sun is represented by θ_z, which is the angle between the direction of the sun and the vertical (see section 4.4.3.3 for more details). The relationship above come from simple geometrical considerations:

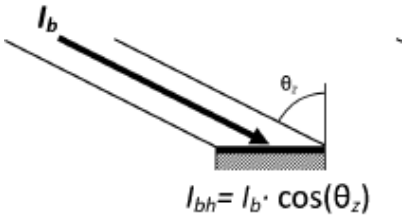

Figure 6: Schematic showing the relationship between direct normal irradiance and beam horizontal irradiance

In the figure, I_b and I_{bh} represent respectively the beam irradiance (another name for DNI) and the

beam horizontal irradiance.

The values of GHI, DHI, BHI and DNI are needed for all the calculations of section 4.5.

In this project, it is always assumed that the global horizontal irradiance (and eventually the diffuse) is always known a priori from measured data. As a consequence, no models to predict these values starting from the extraterrestrial irradiance are treated in this work. It Is worth mentioning that different models exist and more information on these models could be found in [6].

4. Model of the plant with MATLAB

4.1. Methodology

The model created in this project with MATLAB have the purpose of generating the hourly values of several variables of a PV plant starting from hourly values of global horizontal irradiance and temperature and, if available, diffuse horizontal irradiance and wind speed.

For the development of the present model the simulation software PVsyst developed by the university of Genève is taken as the main reference for three reasons. First, because the software is one of the most used in the industry as for example stated in [7]. Therefore, its simulation approach is trusted. Second, because PVsyst has an in-depth approach into the models, providing a high flexibility in the tuning of the parameters of every sub-model, which is precisely one of the goals of the present project. Third, because the authors of PVsyst provide a thorough help manual [8] which explains in details the reasoning behind the models with a pedagogical approach. The software System Advisor Model (SAM) developed by NREL was used as a second reference when the reasoning of PVsyst for some models (e.g. inverter model) could not be found or reproduced. The same reasons listed above are valid for SAM which also provides a well explained manual [9].

The model is structured in different sub-models related to different physical quantities such as plane of array (POA) irradiance current-voltage (I-V) characteristic, temperature of the cell etc. During the development of the MATLAB model, the manuals of the software PVsyst and SAM were consulted as guidelines [8], [9]. The books or articles cited by these manuals were carefully analyzed to obtain the equations used in each particular model and implemented in MATLAB. Numerical algorithms needed to solve the equations were implemented independently since the sources usually deal only with analytical equations. For example, this was the case of the solver for systems of non-linear equations used in the IV curve developed in section 4.6.2.

Each of the sub-models was validated comparing the hourly results of the software developed with results of either PVsyst or SAM, depending on which software the sub-model was based on. In addition, a validation of the whole model from measured irradiance to energy injected to the grid was performed. Results of the validations can be found in section 5.

4.2. Model scope

The models for the following quantities are inside the scope of the project:

1. Diffuse horizontal to Global horizontal ratio (Erb's correlation)
2. Position of the sun (Azimuth and Zenith)
3. Angle of incidence between sun and module
4. POA Incident beam irradiance

5. POA incident sky and ground diffuse irradiance
6. IAM factor for beam irradiance
7. Effective POA global irradiance
8. IV model reference parameters $I_{L,ref}$, $I_{0,ref}$ and $R_{s,ref}$ calculated from $R_{sh,ref}$ and a_{ref}.
9. IV model parameters for any temperature and irradiance.
10. Temperature of the cell at any condition
11. Efficiency of the inverter at any voltage and power
12. Thermal losses in DC cables
13. AC cables and transformer losses
14. Automatic design of the layout: number of modules in series and parallel
15. LCOE of the project

All the above mentioned quantities are calculated hourly.

It is out of the scope of this project:

1. The synthetic generation of weather data from monthly averages.
2. The analysis of soling and spectral losses.
3. The analysis of mismatch losses due to problems in the MPPT.
4. The analysis of reactive and active power in the inverter.

4.3. Weather data and model of diffuse irradiance

4.3.1. Weather data

The weather data that the model can receive as inputs are: the global horizontal irradiance (GHI), the diffuse horizontal irradiance (DHI), the ambient temperature and the wind speed. These weather data are the main input of the model: ambient temperature and GHI are essential for the execution of the software. Wind speed is optional, as explained in section 4.7. Ideally, also data for DHI are needed, however they are not always available: in this case the Erb's model is used to estimate the diffuse irradiance from global irradiance through the clearness index as explained in section 4.3.2. In the present project, it is assumed that at least ambient temperature and GHI are always available as hourly measured values.

4.3.2. Model of the diffuse horizontal irradiance: The Erb's correlation

The Erb's correlation is used to find a ratio between diffuse horizontal irradiance and global horizontal irradiance as a function of the clearness index. The relationship is taken from [6], based on the original study [10], which is the same used by PVsyst [8], and is given by:

$$\frac{DHI}{GHI} = \begin{cases} 1.0 - 0.09\,k_T, & k_T \leq 0.22 \\ 0.9511 - 0.1604k_T + 4.388k_T^2 - \\ \quad -16.638k_T^3 + 12.336k_T^4 & 0.22 \leq k_T \leq 0.80 \\ 0.165, & k_T > 0.8 \end{cases} \quad (4.1)$$

Where $k_t = GHI/I_{0h}$ is the clearness index from equation (3.4.

When plotting equation 4.1 against measured data the correlation is clearly visible (elaborated by the authors of PVsyst [8]):

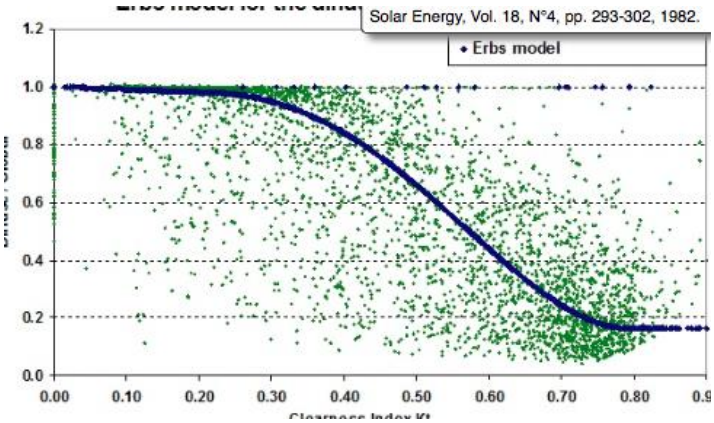

Figure 7: Plot of the Erb's correlation (blue) showing the ratio of DHI/GHI versus the clearness index Kt and the measured DHI/GHI ratio (green). Source [8].

This correlation can be easily understood by looking at the clearness index: the clearness index is the ratio of the irradiance in outer space to the irradiance on Earth's surface (GHI), therefore it is a mean of representing the transmittance of the atmosphere. A higher clearness index means that a higher portion of the beam in outer space is transmitted on Earth, a lower clearness index means that most of the irradiance is diffracted and reflected by the atmosphere thus resulting in a higher diffuse irradiance on Earth. This is why the Erb's correlation shows that when the clearness index is high, the ratio DHI/GHI is low and vice versa. The Erb's correlation is one of the two possible models used in PVsyst when measured data for DHI. The other model is the Perez model, based on the original study [11], but it is considered less robust and increases only slightly the accuracy [8]. Therefore, in the present project the Erb's correlation is used.

4.4. Model of the solar angles and angle of incidence

This section illustrates the procedure followed to calculate the angle of incidence (AOI) between the direction of the sun beams and the normal to the plane of the module. The models needed to calculate the AOI are: the model of the solar time, the equation of time and the solar angles. This part of the software was based on the equations used by PVsyst [8].

4.4.1. Convention used in the weather data: the time shift

To understand what follows it is important to distinguish between solar and clock time. The solar time is the time used for solar calculations and the solar noon is defined as the moment when the Sun, in its apparent movement, passes exactly due south at the position of the observer. On the other hand, the clock time is simply the time used in everyday life.

The weather data such as the GHI or the ambient temperature are usually given as hourly values and are referred to a specific hour of the clock time. Each value is an average over an interval of one hour and the present project uses the convention that the weather data are assumed to be values at the middle of the hour interval. For example, the GHI corresponding to the hour interval 12-13 is considered to be the GHI reaching the modules at 12:30. This convention is used by most weather centers and is followed by PVsyst [8]. The default convention can be modified by the user: this step is fundamental in case the weather data used another convention because this time difference affects heavily the calculations that follow. Moreover, the weather data refer to the clock time, but the solar time is needed to calculate all the solar angles and the AOI. Therefore, the conversion from clock to solar time is required. To sum up, the program calculates the AOI in three steps: first, it sets the time shift to the default or user-defined convention; second, it converts the clock time to the solar time; third, it calculates the solar angle and AOI based on the solar time.

4.4.2. Model of the solar time

In this section the procedure to convert the clock time to solar time is illustrated. The difference between the solar and the clock time in hours can be expressed in a formula as follows:

$$t_s = t_{cl} - TZ + \frac{\psi_{loc}}{15^\circ} + EOT - DST \tag{4.2}$$

Where TZ is the time zone of the location in hours; ψ_{loc} is the longitude of the location in degrees (East positive), EOT is the equation of time in hours explained in the next section, and DST is the daylight saving time in hours.

The difference between clock and solar time is caused by three main reasons:

1. The clock time refers to a time zone which refers to a specific meridian (for example UTC+1 means longitude=15*E). However, the specific longitude of the location is different from this

standard meridian therefore the solar time (which is referred to the observer local meridian) will be different.

2. The Earth's rate of rotation around the Sun varies during the year, leading to differences on the time at which the Sun is due south. This is expressed by the EOT in section 4.4.2.1
3. The daylight-saving time (DST) might be present in the clock time depending on the region and the season. This is a fictitious shift of time made by the society for energy saving purposes, which clearly does not influence the real position of the Sun. Anyway, in the software, the DST is set to zero by default as it is done in PVsyst (by default the weather data are supposed to come without DST). It could be activated if the weather data are recorded using the DST, or to show the output file with the clock time including DST.

4.4.2.1. The equation of time

The equation of time takes into account that the Earth's rate of rotation around the Sun varies during the year due to the variation of the ellipticity of the Earth's trajectory and the obliquity of the Earth's axis. The EOT can be written in many forms depending on the level of accuracy: for instance the authors of [6] suggest an expansion with 5 terms while PVsyst uses an equation with 6 terms [8]. The equation of PVsyst was adopted in this project. The equation of time in hours is as follows:

$$EOT = 0.0072\cos B - 0.0528\cos 2B - 0.0012\cos 3B - 0.1229\sin B - 0.1565\sin 2B - 0.0041\sin 3B \quad (4.3)$$

Where the year angle $B = 2\pi(n-1)/365$ is the same used in equation (3.2) to calculate the extraterrestrial irradiance.

The equation of time creates a negative or positive difference of some minutes between the clock and the solar time. The figure below shows how the EOT (in minutes) changes over one year.

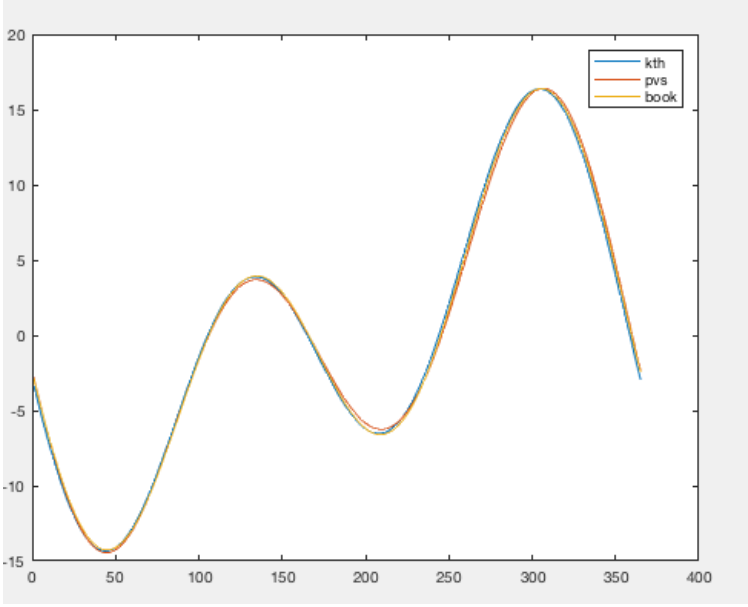

Figure 8: The equation of time (in minutes) for everyday of the year

As it can be seen, the maximum of the EOT is around day 300 (November), for which the solar time is ahead of the clock time by 16 minutes, which is a relatively high number and thus it is important to always consider the EOT when performing solar calculations.

4.4.3. Model of the solar angles

Once the solar time is computed, all the other solar angles are calculated according to the solar time. In this section presents the procedure followed to obtain the solar angles: hour angle, declination, solar azimuth and solar zenith (and altitude). In all the equations and in the software, the angles are in radians.

4.4.3.1. Hour angle

The hour angle represents the position of the sun with respect to the specific location in angles. It can be thought as the angular coordinate of the sun, if its position is projected on the plane of the equator. The hour angle ω, taken from PVsyst manual [8], is given by:

$$\omega = \frac{\pi}{12}(t_s - 12) \tag{4.4}$$

Where t_s is the solar time from equation 4.2.

As it can be seen, the solar hour is zero when it is solar midday, which corresponds to the time at which the Sun is exactly in its highest position in the sky dome at the specific location. The hour angle gains 15 degrees every hour, because the Earth takes 24 hours to complete a rotation around itself, which means it moves at a speed of 15 degrees/hour (360/24=15). This equation is derived from geometrical considerations and is present in any book on the topic, for example [4], [6].

4.4.3.2. Declination

The declination can be seen as the angle between a line that connects the center of the sun with the center of the Earth and the plane of the equator. The formula for the declination δ, which is taken from the PVsyst manual [8] is:

$$\delta = \begin{cases} \operatorname{asin}(\sin(ECL)\sin\left(2\pi\dfrac{n-n_{orig}}{n_{year}}\right)), & n \leq 172 \\ \operatorname{asin}(\sin(ECL)\sin\left(2\pi\dfrac{n-n_{orig}}{n_{year}}\right) + 1.5\sin\left(2\pi\dfrac{n-173}{n_{year}}\right)), & n > 172 \end{cases} \tag{4.5}$$

And:

$$n_{orig} = 79 + \mathrm{MOD}(n, 4)/4 \tag{4.6}$$

Where: ECL is the inclination between Earth's axis and the ecliptic plane equal to 23.444° or 0.40917 radians, n is the day of the year, n_{orig} is the year origin, n_{year} are the days in one year and $\mathrm{MOD}(a, b)$ is the modulo function that represents the remainder of the division of a by b. This last function is needed to take into account that non-leap year can actually be longer than 365 days by quarters of a day, so that in 4 years another day is added obtaining a leap year of 366 days.

Again, other versions of these formulae are possible but it was preferred to follow the approach of PVsyst [8] for consistency.

The declination changes with the day of the year from approx. -23.4 degrees to +23.4 degrees at the winter and summer solstices respectively. The declination is also the main reasons why seasons exist.

4.4.3.3. Sun zenith and azimuth

Sun zenith and azimuth are the two coordinates used to locate the position of the Sun in the sky dome. The zenith is the angle between a vertical line and the direction of the Sun beam. The solar altitude is the complementary angle of the Zenith. The azimuth is the angle between the south and the projection of the Sun on the plane of the location. For a better understanding, the figure below illustrates the two solar angles (together with the of the surface angles and the AOI discussed in the following section):

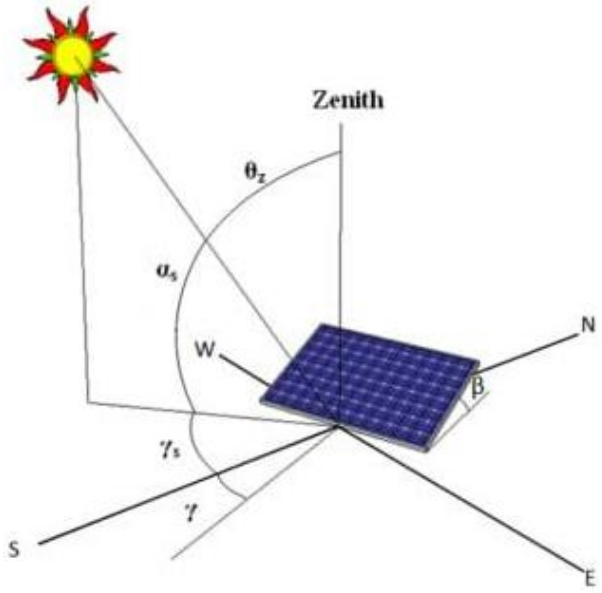

Figure 9 Relevant angles of the position of the Sun, the orientation of the module and angle of incidence (AOI). Source [12].

Looking at the figure above, all the angles can be calculated with geometrical considerations. The zenith θ_z is calculated as:

$$\theta_z = \arccos(\cos\varphi\cos\delta\cos\omega + \sin\varphi\sin\delta) \tag{4.7}$$

And the solar altitude α_s is simply the complementary angle:

$$\alpha_s = \frac{\pi}{2} - \theta_z \tag{4.8}$$

The azimuth γ_s is given by:

$$\gamma_s = \text{sgn}(\omega) \left| \arccos\left(\frac{\cos\theta_z \sin\varphi - \sin\delta}{\sin\theta_z \cos\varphi} \right) \right| \tag{4.9}$$

Where φ is the latitude of the location in radians (positive in the northern hemisphere), δ and ω are respectively hour angle and the declination discussed previously.

These equations are taken from the manual of PVsyst [8]. They are derived from geometrical considerations and can be found in the same formulation in any book about solar photovoltaics, such as [4], [6]. Note that the present program is written considering the solar zenith, while PVsyst uses the solar altitude, so the cosines and sines are inverted since they are complementary angles. This is just a matter of choice and the results are anyway equivalent.

4.4.4. Model of the angle of incidence between sun and panels

To calculate the angle of incidence (AOI) between the direction of the beams and the plane of the module, two more angles (see Figure 9) defining the orientation of the module need to be specified:

1. The tilt angle θ_t of the module, which represent the angle between the plane of the module and the ground
2. The azimuth γ_m of the module: angle between the orientation of the panel and due south.

With these two angles, and the two coordinates of the position of the Sun, the angle of incidence can be finally calculated as:

$$\theta_{AOI} = \arccos(sin\theta_t \sin\theta_z \cos(\gamma_s - \gamma_m) + cos\theta_t \cos\theta_z) \tag{4.10}$$

Again, the formula above is derived from geometrical considerations, and therefore can be found in any book about this topic, such as [4], [6].

4.5. Model of the effective incident irradiance on the module

The incidence irradiance is the amount of solar energy that effectively reaches the cells of the module. It is the main input of the model it affects almost linearly the power output of the modules. The following graph shows how a generic IV curve changes under different irradiances:

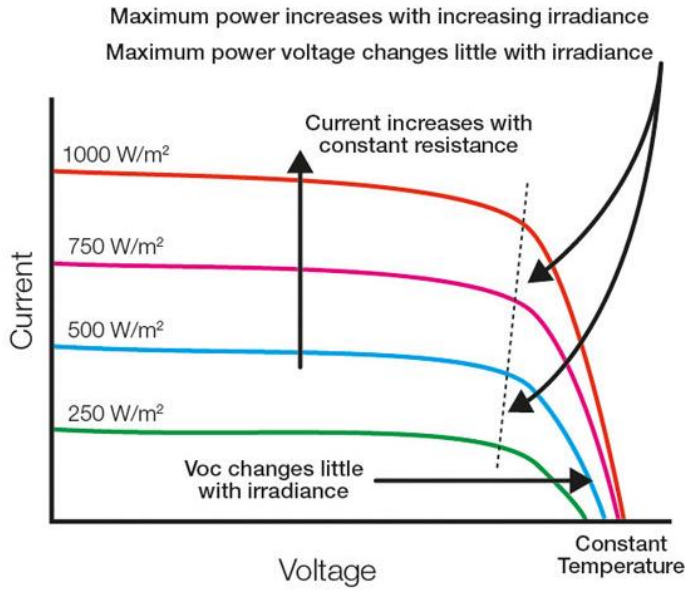

Figure 10 Effects of the irradiance on the IV curve of a generic module. Source [13].

As shown above, the IV curve varies heavily with irradiance. The maximum power point varies almost linearly with the irradiance and is clearly higher for higher irradiances (see Section 4.6.4), while the voltage of the maximum power point increases only slightly.

4.5.1. Steps needed to calculate the incidence plane of array (POA) irradiance

The software calculates the hourly effective plane of array (POA) irradiance with the following steps:

1. The POA beam irradiance is calculated with the angle of incidence (AOI).
2. The POA ground-diffuse irradiance is calculated.
3. The POA sky-diffuse is calculated with Hay model.
4. The Incident Angle Modifier (IAM) is calculated on the beam component with the AOI.
5. The IAM factors for sky and ground diffuse is taken from a table given the array tilt.
6. The effective POA irradiance is found multiplying each component by its IAM loss.

Note that the approach followed here does not include an analysis of the self-shading due to adjacent rows which is present in large scale solar PV plants but could not be implemented in this project due to time and resources constrains. Nevertheless, it could be an interesting further study as discussed in Section **¡Error! No se encuentra el origen de la referencia.**.

4.5.2. Model of the incidence plane of array (POA) irradiance

It is important to calculate the POA irradiance because the panels have a fixed tilt, therefore the part of irradiance that is actually reaching the cells is going to be less than the total available irradiance as it varies with the AOI varies: when the sun is low, e.g. at sunset and sunrise, the available irradiance is lower. The POA irradiance can be thought of being composed by three parts: beam, sky-diffuse and ground-diffuse:

$$E_g = E_b + E_{sd} + E_g \tag{4.11}$$

Where $\mathrm{E_b}$ is the POA beam irradiance, $\mathrm{E_{sd}}$ is the POA sky-diffuse irradiance and $\mathrm{E_g}$ is the POA ground-diffuse irradiance.

The equation 4.10 represents only the irradiance reaching the surface of the module, without considering the optical losses considered in the effective POA irradiance in Section 4.5.8.

4.5.3. Model of the POA beam irradiance

The POA beam irradiance is the part of the beam irradiance that reaches the plane of the array. It is calculated by simply considering the projection of the DNI on the plane of the array by means of the cosine of the angle of incidence. This is a geometrical transposition and therefore does not imply any particular assumption. The same equation can be found in both SAM and PVsyst and all the consulted sources [4], [6], [8], [9]. The beam irradiance E_b effectively reaching the surface of the panel is given by:

$$E_b = DNI \cos\theta_{AOI} \tag{4.12}$$

Where DNI is the direct normal irradiance in and θ_{AOI} is the angle of incidence AOI.

4.5.4. Model of the POA ground diffuse irradiance

The POA ground diffuse is the part of the ground diffuse irradiance that reaches the array. It is calculated assuming that a part of irradiance reaching the Earth's surface is reflected in an isotropic way. Since it is reflected equally in any direction, the portion of this irradiance that reaches the module can be calculated by mean of the view factor ($1 - \cos(\theta_t)/2$) from the ground to the panel [6]:

$$E_g = GHI * \rho \frac{1 - \cos(\theta_t)}{2} \tag{4.13}$$

Where GHI is the global horizontal irradiance in W/m^2, ρ is the albedo of the ground and θ_t is the tilt of the module.

The albedo is a factor that varies from 0 to 1 indicating the portion of irradiance that is reflected from the ground, different kind of soils might have different values. The default value used in PVsyst, and SAM is 0.2 [8], [9]. The same value will be used in the present project as a default value.

The factor $1 - \cos(\theta_t)/2$ represents the view factor from the ground to a tilted surface. It is

calculated following the methodology explained in a study dedicated specifically on calculations of the view factors needed in PV systems [14]. According to this study, the view factor between two surfaces A1 and A2 is defined as:

$$F_{12} = \frac{Diffuse\ energy\ from\ A_1\ that\ reaches\ A_2}{Total\ diffuse\ energy\ from\ A_1} \tag{4.14}$$

This model is used in PVsyst and in SAM as the default and only model [8], [9]. Therefore, it was used also in this project.

4.5.5. Model of the POA sky diffuse irradiance

The POA sky diffuse is the part of the sky diffuse irradiance that reaches the array. It is calculated under the assumption that the diffuse irradiance from the sky is composed by an isotropic part (coming from all directions) and a circumsolar part which is aligned with the direction of the beam irradiance. To evaluate how much of the sky diffuse irradiance reaches the array, the isotropic part is multiplied by the view factor while the circumsolar part is multiplied by the cosine of the angle of incidence (as the calculations done for the beam irradiance). This model was developed by Hay-Liu and it is widely used. The effective sky-diffuse irradiance E_{sd} is given by [8]:

$$E_{sd} = DHI\left[k_b \cos(\theta_{AOI}) + (1 - k_b) + \left(\frac{1 + \cos\theta_t}{2}\right)\right] \tag{4.15}$$

Where: DHI is the diffuse horizontal irradiance, K_b is the beam clearness index (defined in section 3.1), θ_{AOI} is the angle of incidence and θ_t is the tilt of the module.

In this model, the sky diffuse irradiance is thought as having two different parts, an isotropic part and an anisotropic part (first term) that is the diffuse irradiance around the sun's disk. This last part is considered to come aligned with the beam irradiance, therefore its transposition on the array plane is the same as the one done for beam irradiance. On the other hand, the isotropic part is thought as coming homogeneously from the sky and the term $(1 + \cos\theta_t)/2$ represents the view factor between the panel and the sky and it is calculated following the study described in 4.5.4.

The ratio between the circumsolar and the isotropic part is found by means of the beam clear index $k_b = DNI/E_a$ introduced in Section 3.1. k_b is the ratio between the direct normal irradiance and the extra-terrestrial beam irradiance: it is a measure of the transmittance of the atmosphere for the beam component. The higher Kt, the clearer the conditions of the sky and the higher the proportion of the sky-diffuse that is considered circumsolar. On the other hand, if Kt is low, it means that the beam irradiance that reaches the Earth, is much lower than the one from the space and therefore

the sky-diffuse is considered to be composed mainly of isotropic diffuse. More details are found in Section 3.1

There are other models for the transposition of the sky-diffuse component on the plane of array, such as the Perez model or the Hay, Davies, Klucher, Reindl (HDKR) sky diffuse model [6]. The present project uses the Hay-Liu model presented above for the following reasons. It was the main model used in PVsyst till 2015, because more complexes models such as the Perez model would improve only slightly the accuracy while increasing the complexity. Moreover, the authors of PVsyst state that the Perez model is less robust as much more sensible to the accuracy of the measured data. Therefore, the Hay-Liu model is used in this project.

4.5.6. Model of the Incident Angle Modifier (IAM) for the beam component

The incident angle modifier (IAM) is an optical loss that considers that a part of the incoming beam irradiance is reflected away by the module, and does not reach the cell. The IAM is defined as the ratio between the transmittance at the specific AOI and the transmittance at AOI=0. The present project uses the parametrization ASHRAE 93-3003:

$$IAM = 1 - b\left(\frac{1}{cos\theta_{AOI}} - 1\right) \tag{4.16}$$

Where b is a unitless fitting parameter and θ_{AOI} is the angle of incidence.

The equation is a parametrization to obtain a simple fit with just the parameter b. Physically, the principle is described by Fresnel's Law of reflection between two different media. The parameter b is set to 0.05 as a default, following the default of PVsyst.

The higher the AOI, the higher the IAM losses as shown by the figure below:

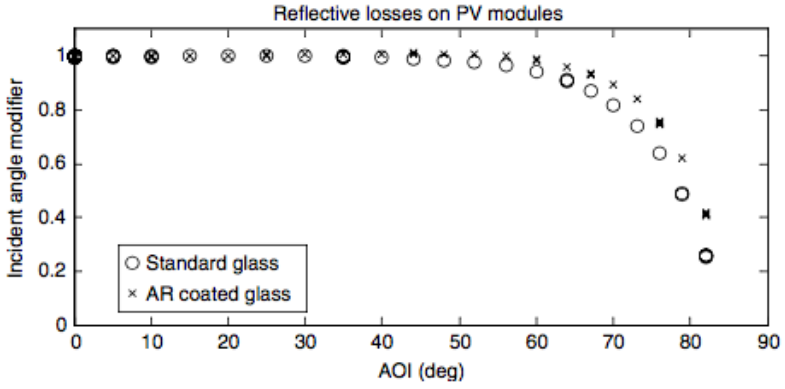

Figure 11 Beam IAM losses for different angles of incidence (AOI) as calculated with ASHRAE 93-3003. Source [4]

This model was used as it is the default model because it is the default model used in PVsyst [8], and because it is a standardized and simple model.

4.5.7. The incident angle modifier (IAM) for ground and sky diffuse

The IAM for the diffuse irradiance follows the same principles as IAM for the beam irradiance, with the difference that the diffuse beams could come from any direction (here both ground and sky-diffuse are considered to be isotropic). For this part, the same reasoning of PVsyst was followed, but for sake of simplicity, since the IAM factors are considered to be constant given a tilt, the present model does not compute the IAM in every simulation, instead it uses tabulated values that were extrapolated from a batch simulation performed in PVsyst for different tilt angles.

To get this data, PVsyst performs the integral of the function for the IAM losses described in equation (4.16) considering a beam that comes in all the possible directions from the sky according to the isotropic model of sky-diffuse. The same reasoning applies to the ground-diffuse. The results can be visualized in the following graphs which are taken from the detailed loss section of PVsyst [15]:

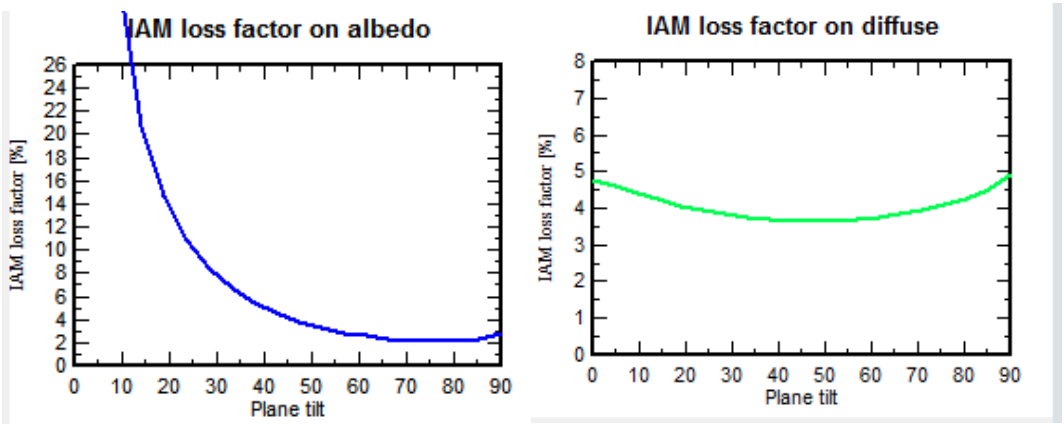

Figure 12 Sky-diffuse and ground diffuse IAM losses versus plane tilt of the module. Source PVsyst software [15]

As it is shown, the IAM loss factor for ground-diffuse increases exponentially when the AOI decreases while the IAM loss factor for sky-diffuse behaves almost symmetrically always between 4-5%. It should be noted that losses in ground-diffuse do not have a big impact in the overall system because ground diffuse accounts for the smallest part of the effective irradiance.

4.5.8. Model of the effective plane of array irradiance (before shading)

The effective plane of array irradiance is the irradiance that actually reaches the surface of the PV cells inside the module. It is the irradiance that will produce the photovoltaic effect, and will be the input for the IV model. The effective POA irradiance is calculated without considering shading as discussed in Section 4.5.1. The effective POA irradiance E_g can be expressed as the sum of the three components of the incident POA irradiance multiplied by its respective IAM factor as calculated in the previous sections:

$$E_g = SF(E_b IAM_b + E_{sd} IAM_{sd} + E_g IAM_g) \quad (4.17)$$

Where SF is the soling factor, E_b is the POA beam irradiance, E_{sd} is the POA sky-diffuse irradiance and E_g is the POA ground-diffuse irradiance. IAM_b, IAM_{sd} and IAM_g are the IAM loss factors for beam, sky-diffuse and ground-diffuse.

In the equation above, the only new parameter is the soling factor which considers losses due to dirt on the panel. It is very challenging to accurately predict this factor, as it varies with wind speed, precipitations, specific location, humidity etc. For this reasons in the present project this factor was excluded from the analysis and it is set to 1 by default.

4.6. Model of the module I-V curve

A model of the current-voltage (I-V) curve of the PV module is fundamental as it determines how much power can be generated by the module under any working condition. The power that can be extracted from a PV module varies with irradiance (Figure 10), temperature (Figure 16) and the working point of the I-V curve. Therefore, to perform the simulation and calculate the power produced and the energy yield it is necessary to find a model that can create the I-V curve given any external conditions of irradiance and temperature. When the I-V curve is known and the working point is known, the power can be calculated at any moment by multiplying current and voltage. The present project considers that the working point is always the maximum power point (mismatch losses are out of the scope).

The following sections introduce the single diode model, the procedure used to solve the I-V curve with this model and the assumptions on the model parameters needed to compute the I-V curve when measured data are not available.

4.6.1. The single diode model of the IV curve of a PV module

The single diode is a model in which the PV cell is modelled as a current source I_L with a reverse diode with current I_d, a shunt (parallel) resistance R_{sh} and a series resistance R_s. The equivalent electrical circuit is shown below:

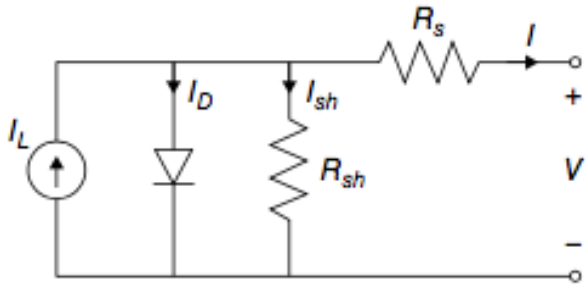

Figure 13 Equivalent electrical circuit of the single diode model. Source [4]

Given the circuit above, at a fixed temperature and irradiance, the current flowing out of the system is described by the following equation:

$$I = I_L - I_0 \left[\exp\left(\frac{V + IR_s}{a}\right) - 1\right] - \frac{V + IN_sR_s}{R_{sh}} \tag{4.18}$$

With the parameter a defined as:

$$a = \frac{nkTN_s}{q} \tag{4.19}$$

Where I_L is the photo-generated current (A), I_0 is the diode saturation current (A), V is the module voltage (V), R_s is the series resistance (Ω), n is the diode ideality factor (also called gamma), N_s is the number of cells in series per module, R_{sh} is the shunt resistance (Ω), T is the temperature of the cell, k is the Boltzmann's constant ($1.381 \times 10^{-23}\, J/K$) and q is the electron charge (1.602×10^{-19} °C). The parameter a is defined for simplicity.

The equation (4.18 is found solving the circuit above for the output current I. The current I is found as the photo-generated current I_L minus the current flowing in the diode (second term) and the current flowing in the shunt resistance (third term). This is an implicit non-linear equation that must be solved at any condition of temperature and irradiance. The detailed process on how to solve is explained in sections 4.6.2, 4.6.3 and 4.6.4.

In the literature, there are several models to describe the I-V curve of a solar panel, the single diode is applied in many of the available PV modeling software: it is the default model in PVsyst and is available as a model in SAM. Others use a much simpler approach, in which the IV curve is not calculated, and the power is calculated through the temperature coefficient of maximum power point, explained for example in [6]. Others use approaches that calculate the I-V curve only in 5

points. More accurate models exist, like the 2 diodes models [16]. However, the approach followed by PVsyst is to use the one diode model, and vary the value of the ideality factor to represent the effect of two different diodes [8]. The authors claim that a more complex model is not needed as the level of accuracy of the parameters from the manufacturers is not very high, and therefore a high accuracy model would not lead to significant improvements. For these reasons, the single diode model is implemented in this project.

4.6.2. Methodology to solve the IV curve

In the following sections, a method to solve the IV equation is presented, the method is based on the procedure described in [6] with adjustments from the manual of PVsyst [8] and further information based on studies describing the IV model used in PVsyst [7], [17], [18]. Equation (4.18 represents the relationship between current and voltage of a module at a fixed temperature and irradiance. To solve for the current, 5 parameters are needed: I_L, I_0, n, R_s and R_{sh}, which means that in principle 5 equations are necessary to have a determined solution. The equation (4.18 describes the system at fixed temperature and irradiance with a set of 5 parameters, which means that at any new condition of T and G, the 5 parameters must be recalculated.

The method presented here is composed of two steps: first, solving a system of equations to find the unknown parameters at reference conditions (T=25C and G=1000) as presented in section 4.6.3 and then calculating the parameters at different temperature and irradiance as in explained in 4.6.4.

4.6.3. Calculation of the IV parameters at reference conditions

In this section, the parameters of the equation (4.18 at reference condition are calculated (from now on referred to as reference parameters). In everything that comes next, the irradiance and the temperature of the cell is supposed to be known at standard conditions. In addition, from the PV module datasheet, the following parameters are considered to be known at standard conditions: V_{OC}, I_{SC}, I_{mpp}, V_{mpp} and μ_{Isc}, respectively voltage at open circuit condition, short circuit current, voltage at maximum power point, current at maximum power point, and temperature coefficient of the short circuit current. These parameters are always available in PV datasheets.

The equation of the IV curve present 5 unknown parameters, so in principle 5 equations are needed. The procedure described in [6] suggests to create the system by finding 5 conditions from the PV datasheet. The first three conditions are the known points of the IV curve: short circuit current, open circuit voltage and voltage and current at maximum power point. The fourth condition is setting the derivative of I-V curve equal to zero in its maximum in the known maximum power point. The fifth condition is setting the derivative of the open circuit voltage equal to the temperature coefficient of the open circuit voltage. These five conditions result in the following set of equations:

$$I_{sc,ref} = I_{L,ref} - I_{0,ref}\left[\exp\left(\frac{I_{sc,ref}R_{s,ref}}{a_{ref}}\right) - 1\right] - \frac{I_{sc,ref}R_{s,ref}}{R_{sh,ref}} \quad (4.20)$$

$$I_{L,ref} = I_{0,ref}\left[\exp\left(\frac{V_{oc,ref}}{a_{ref}}\right) - 1\right] + \frac{V_{oc,ref}}{R_{sh,ref}} \quad (4.21)$$

$$I_{mp,ref} = I_{L,ref} - I_{0,ref}\left[\exp\left(\frac{V_{mp,ref}+I_{mp,ref}R_{s,ref}}{a_{ref}}\right) - 1\right] - \frac{V_{mp,ref}+I_{sc,ref}R_{s,ref}}{R_{sh,ref}} \quad (4.22)$$

$$\frac{I_{mp,ref}}{V_{mp,ref}} = \frac{\frac{I_{0,ref}}{a_{ref}}\exp\left(\frac{V_{mp,ref}+I_{mp,ref}R_{s,ref}}{a_{ref}}\right) + \frac{1}{R_{sh,ref}}}{1 + \frac{I_{0,ref}R_{s,ref}}{a_{ref}}\exp\left(\frac{V_{mp,ref}+I_{mp,ref}R_{s,ref}}{a_{ref}}\right) + \frac{R_{s,ref}}{R_{sh,ref}}} \quad (4.23)$$

$$\frac{\partial V_{oc}}{\partial T} = \mu_{v,oc} \cong \frac{V_{oc}(T_c) - V_{oc}(T_{c,ref})}{T_c - T_{c,ref}} \quad (4.24)$$

Where the variables with the subscript 'ref' are at reference conditions of T=25°C and G=1000W/m^2: $I_{sc,ref}$ is the short circuit current (A), $I_{L,ref}$ is the photo-generated current (A), $I_{0,ref}$ is the diode saturation current (A), $R_{s,ref}$ is the series resistance (Ω), a_{ref} is the parameter defined above in equation (4.19), $R_{sh,ref}$ is the shunt resistance (Ω), $V_{oc,ref}$ is the open circuit voltage (V), $I_{mp,ref}$ is the current at maximum power point (A), $V_{mp,ref}$ is the voltage at maximum power point (V), μ_{Voc} is the temperature coefficient of the open-circuit voltage (V/°C) and $T_{c,ref}$ is the temperature of the cell (°C).

In theory, solving simultaneously this set of equations should provide the five parameters at reference conditions. However, in the manual of PVsyst, the authors, referring to this approach, suggest to avoid using all the five equations to solve the system because it would often lead to solution with no physical meaning as the parameters could be out of their physical range, (e.g. the ideality factor greater than 2 etc). The authors of PVsyst suggest instead to limit the number of unknowns by setting $R_{sh,ref}$ to a default value (which might be changed or measured as explained in 4.6.4 and 4.6.6), and guessing $R_{s,ref}$, thus remaining with only 3 unknowns: $I_{L,ref}$, $I_{0,ref}$ and n and using only the first three equations above to solve the system [8], [18]. Once the system is solved, PVsyst proposes different ways to find the actual $R_{s,ref}$ as explained in section 4.6.4. This project follows the same method as PVsyst as it is proven that achieve great accuracy [6] thus leading to a system composed by only the three equations from (4.20) to (4.22).

To solve this system of three nonlinear equations, different numeric methods could be used such as Newton method for systems, but for the sake of simplicity, the inbuilt MATLAB function fsolve will be used, also because which proved to be rapid and effective when running the program.

To reduce the computational time when solving such a complex nonlinear system, an accurate initial guess for the variables is needed. The authors of [6] provide a guideline on how to guess the parameters:

1. $I_{L,ref,guess}$ is guessed to be equal to Isc because at short circuit condition the other two terms of the equation are very small:

$$I_{L,ref,guess} = I_{sc,ref} \tag{4.25}$$

2. $I_{0,ref,guess}$ is guessed by neglecting the last term and the -1 from the equation at open voltage (eq. (4.21):

$$I_{0,ref,guess} = I_{sc,ref} \exp\left(\frac{-V_{oc,ref}}{a_{ref,guess}}\right) \tag{4.26}$$

3. $R_{s,ref,guess}$ is guessed by inserting all the guess values in the equation at maximum power point (eq. (4.22) neglecting the last term and the -1:

$$R_{s,ref,guess} = \frac{a_{ref,guess}\left(\log\left(\frac{I_{L,ref,guess} - I_{mp,ref}}{I_{0,ref,guess}}\right) - V_{mp,ref}\right)}{I_{mp,ref}} \tag{4.27}$$

With the above guesses the system can always be solved smoothly and with a limited amount of computational power. Note that the unknown parameters need to be found only once per panel, and then they are saved in the software. Instead, for the parameters at any T and G, that need to be calculated hourly, there is no need to solve the nonlinear system again. In facts, the parameters just need to be recalculated according to the specific T and G, which does not imply solving a system, but only simple equations and the implicit I-V equation as explained in section 4.6.4. Therefore, the resulting computational load and time is not particularly heavy and a whole simulation, that calculates I-V curves and working points every hour, can be performed in less than 25 seconds (depending on the CPU of the computer).

4.6.4. Calculation of the IV parameters at any given temperature and irradiance

In this section, the method to find the 5 unknown parameters: Rs, Rsh, Gamma, Iph, Io of the single diode model at any temperature and irradiance is illustrated. It is assumed that the value of Rs is

independent of temperature and irradiance, as assumed by [6] and PVsyst [9]. The other parameters are calculated with equations that relate the reference value of the parameter with the new value of the parameter as a function of irradiance or temperature (or both).

4.6.4.1. The photo-generated current

The photo-generated current is a function of the irradiance and the temperature given by:

$$I_L(G,T) = \frac{G}{G_{ref}}\left[I_{L,ref} + \mu_{Isc}(T - T_{ref})\right] \tag{4.28}$$

Where: G is the irradiance in W/m^2, G_{ref} is the irradiance at standard conditions (1000 W/m^2), μ_{Isc} is the temperature coefficient of the short circuit current (°C/A).

The photo-generated current is proportional to the incoming irradiance, and increases slightly with temperature (the value of the temperature coefficient on short circuit current is of the order of 0.05%/C).

4.6.4.2. The diode reverse saturation current

The diode reverse saturation current varies only with temperature according to:

$$I_0(T) = I_{0,ref}\left(\frac{T}{T_{ref}}\right)^3 \exp\left[\frac{q\varepsilon_G}{nk}\left(\frac{1}{T_{ref}} - \frac{1}{T}\right)\right] \tag{4.29}$$

Where ε_G is the bandgap equal to 1.12eV for crystalline silicon.

The above two equations are taken from [6] and are the same used in PVsyst [8]. Note that in [6] the authors propose an equation to vary ε_G according to the temperature, instead in PVsyst ε_G is considered to be constant [8]. The approach of PVsyst was followed, also because the variation of ε_G is anyway very small and its impact on the IV curve is negligible.

4.6.4.3. The shunt resistance

For the shunt resistance, the authors of PVsyst propose an empirical model introduced with an experimental study [18] and further discussed by other authors [7]. Following this approach, the shunt resistance is modeled as having an exponential behavior:

$$R_{sh}(G) = R_{sh,base} + \left(R_{sh,0} - R_{sh,base}\right)\exp\left(-R_{sh,Exp}\left(\frac{G}{G_{ref}}\right)\right) \tag{4.30}$$

And:

$$R_{sh,base} = max\left[\left(\frac{R_{sh,ref} - R_{sh,0}\exp\left(-R_{sh,exp}\right)}{1 - \exp\left(-R_{sh,exp}\right)}\right), 0\right] \quad (4.31)$$

Where: $R_{sh,0}$ and $R_{sh,base}$ are empirical parameters in Ω.

The above equation models the shunt resistance R_{sh} as having an exponential increase at low irradiances. Recalling that a higher R_{sh}means less losses, this adjustment increases the efficiency at low irradiances, and overall increases the accuracy of the IV model [18]. The exponential behavior of R_{sh} when varying the irradiance, is illustrated below from [18]:

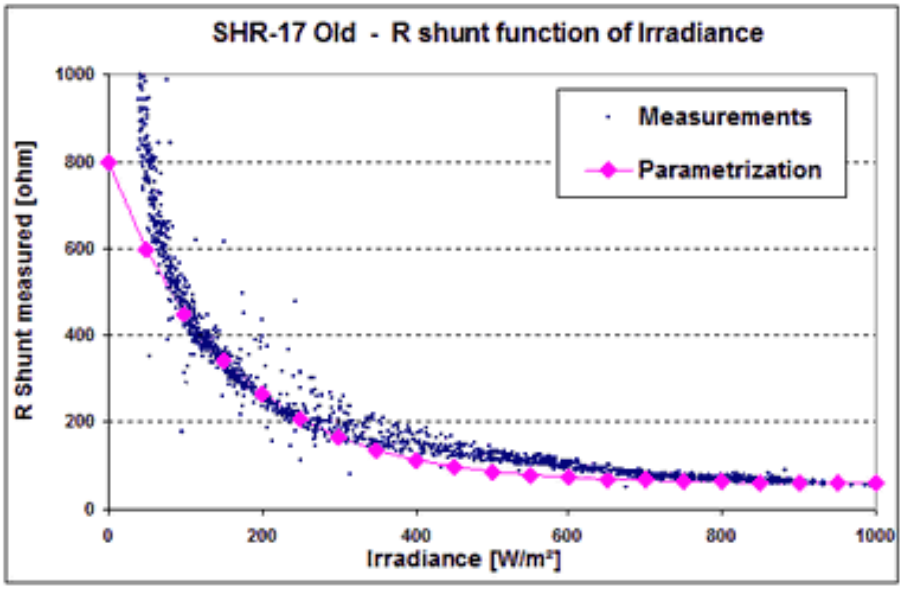

Figure 14 Shunt resistance as a function of the irradiance. Source [18].

4.6.4.4. The ideality factor gamma

For the ideality factor gamma, the default approach of PVsyst was to consider it constant and independent of temperature and irradiance [8]. Later, they introduced an empirical parameter μ_γ to vary gamma with temperature so that the derivative of the maximum power point with respect to the temperature can be adjusted with the temperature coefficient of Pmp provided by the manufacturer datasheet as explained in PVsyst manual [8] and further discussed in [17]. In the present project, the value of μ_n is not calculated but can be inserted externally to be a model parameter of the module. The reasoning performed by PVsyst is anyway explained for a better understanding. According to this approach, gamma varies with temperature according to:

$$n(T) = n_{ref} + \mu_n(T - T_{ref}) \quad (4.32)$$

The adjustment can be understood visually by looking at:

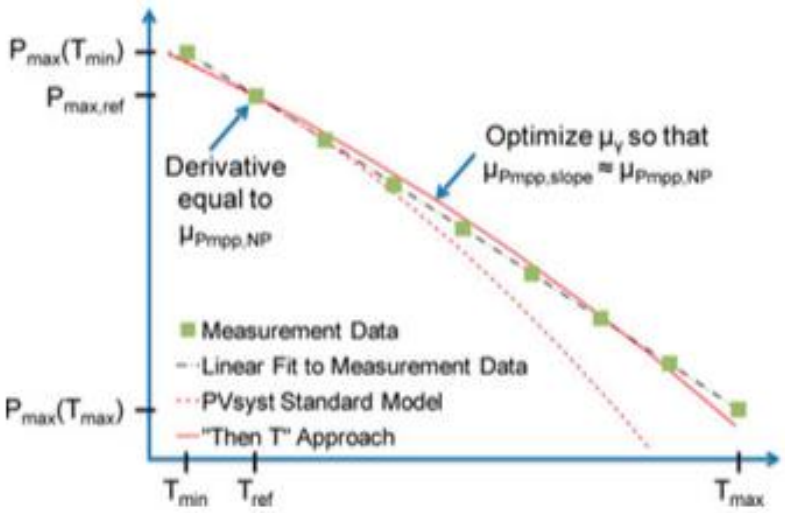

Figure 15 Maximum power as a function of the temperature for three different models and comparison with measurement data. Source [17]

Where $\mu_{Pmpp,NP}$is the value of the datasheet and $\mu_{Pmpp,Slope}$is the value of the model.

The authors of PVsyst warn that the value of the μ_{Pmpp} provided in the datasheet of the modules might not be representative of the behavior of the module in real conditions, because the manufacturers provide just one value of μ_{Pmpp} usually measured at 25 C, while instead it itself changes with temperature. Therefore, in PVsyst the correction of gamma to obtain the same μ_{Pmpp} as the one in the datasheet is an option of the user. The same approach was followed in the developing of this software, if the value of μ_{Pmpp} can be found in an external database, which is usually possible for example from SAM and PVsyst that provide an update database of modules.

4.6.5. Calculation of the IV curve and maximum power point given all the parameters

In this section, the method to calculate the points of the IV curve and the maximum power point is presented. Once all the parameters of the IV curve are calculated at the specific temperature and irradiance (as explained in section 4.6.4), IV equation is finally fully described. Still, the single diode equation (4.18) is an implicit equation, because the current appears in both sides of the equation, therefore it cannot be solved analytically. In the present project this equation is solved numerically through a simple Newton Method taken from [19], that was chosen because it has proven to converge to a solution in few cycle and with limited computational time.

To find the I-V curve and the maximum power point, the algorithm used proceeds in the following

way. First, an equally spaced vector of voltage from 0 to Voc is generated, then the newton method finds for each voltage the corresponding current by iterating till the difference between two steps is smaller than a given tolerance. Second, only the positive values of the current are kept with their respective voltage: the two vectors of voltage and current fully describe IV curve. Third, to find the power, the values of the vectors of voltage and current are multiplied. Finally, the maximum power point is the calculated as the numerical maximum of the power vector. Moreover, the program saves also Imp and Vmp, respectively current and voltage corresponding to the maximum power point needed for the calculation of the inverter losses and the losses in the DC cables discussed in sections 4.9 and 4.10.1 respectively.

In this project, the array is supposed to work always at maximum power point thanks to the MPPT. Therefore the Pmp, Imp and Vmp found above are considered to be the output of a module of a string. Sequentially, they are then multiplied by respectively the number of modules in an array, the number of modules in parallel, and the numbers of module in strings to obtain the power, current and voltage of the array as discussed in section 4.8.1. These values will be the input of the inverter model 4.9.

Note that in this procedure, the maximum power, current and voltage were calculated through the maximum of a numeric array. One could claim that this reduces the accuracy to the number of equally spaced points previously defined for the voltage vector chosen at the beginning. And for example, in [6] the authors present an analytical way to find the maximum working point. However, calculating the maximum power point analytically would add unnecessary computational power because the software already produces results with a root mean square error compared to the DC power of PVsyst lower than 0.27% as explained in section 5. Lastly, for this procedure, an explicit algorithm from PVsyst has not been found, therefore the algorithm explained above was chosen due to its high accuracy and low computational power.

4.6.6. Assumptions on the parameters of the IV curve and methods to find them experimentally.

This section is divided in two parts, the first one introduces the assumptions made to set default parameters for the I-V model when only the data from datasheet are available and the second part briefly shows possible methods to find these parameters experientially.

As explained in section 4.6.3, to calculate the single diode model and the I-V equation at standard conditions, 5 parameters are needed: *Rsh, Rs, n, Iph, Io.* However, since *Rs, Ioh* and *Iph* and Io are calculated with the resolution of the system, only two parameters are needed: gamma and *Rsh*. In addition, to calculate how these parameters vary with temperature and irradiance as shown in section 4.6.4, other two parameters are needed: Rsh_{exp} and Rsh_0. Therefore, a total of four parameters: gamma, *Rsh,* Rsh_{exp}, Rsh_0, must be either assumed or measured for the model to work properly.

If the only available data are the one from the manufacturer datasheet, the parameters will be assumed following the same assumptions used in PVsyst, given their extensive experience in the field and continuous updating to new technologies.

For the value of gamma, the default value will be n=1.05 for mono-crystalline and 1.1 for polycrystalline as considered in PVsyst [8].

For the *Rsh*, if an IV curve is available, it could be calculated as the inverse of the slope of the I-V curve at short circuit, but it is not implemented in the model (the operation should be performed graphically). Otherwise, the method to find the default value proposed by PVsyst equal to 400Ω will be used for crystalline silicon.

The value of Rsh_{exp} is set equal to 5.5 as the authors of PVsyst say it produces good results for almost all the modules they have tested [8], [18].

The value of Rsh_0 is set as $Rsh_0 = 4 * Rsh_{ref}$ as suggested by the authors of PVsyst, even though they add a notice to explain that computing this ratio with great accuracy is problematic because of complications in the measurements of the slope of the IV curve at low irradiances [8].

The assumptions considered above are needed if the only available data is from the module datasheets. On the other hand, if experimental tests could be performed on the module to measure its IV curve at different conditions, there are different methods to calculate the parameters so that the produced IV curve has the closest fit to the measured data. This alone is an extensive topic and it is out of the scope of the present project. Nevertheless, during the development of the present project, two possible methods to perform this optimization were found and are mentioned here for the interest of the reader. The first one proposes a method based on a numerical optimization which finds the set of reference parameters that best fits their measured data at different irradiance [7]. The second one builds up on the first one and continues a similar study not only limited at varying the irradiance but also varying the temperature and compares different modeling approaches [17]. Clearly, the computational power increases with the complexity of the optimization algorithm, but this might be justified in an advanced phase of modeling of a project in which few possible PV panel models were selected and an accurate simulation is needed to assess the different characteristics with high accuracy. However, in the present model the assumptions made above already constitute an accurate model and anyway all the parameters can be changed by the user. Therefore, if more accurate assumptions of the parameters were available, they could be inserted in the model.

4.6.7. Summary of the steps needed to calculate the hourly power generated with the single diode model of the IV curve

In this section, a summary of the necessary steps to obtain the hourly maximum power point generated by the PV panel through the single diode model is presented. The steps are as follows:

Steps that are computed once for PV module model:

1. A PV module is chosen with at least the following information: *Impp, Vmpp, Isc, Voc muIsc* at T=25C and G=1000W/m^2, Ns, and the cell area Ac.
2. In case the parameters to model the IV curve are available from a database, skip to step 7.
3. Rsh and gamma are guessed as explained in 4.6.6.
4. The system of 3 nonlinear equations is solved to obtain the 3 missing parameters I_L, Io and Rs at reference conditions according to 4.6.3.
5. The set of reference parameters is saved in a struct and it is linked to the struct of the module.

Steps that are computed every hour:

6. The 5 parameters are calculated with the specific temperature and irradiance, as explained in 4.6.4.
7. The IV curve is calculated in each point, current and voltage are saved in vectors. The power is found as element-by-element multiplication of the two according to 4.6.5.
8. The output DC power, voltage and current of the module are calculated as the numerical maximum of the power *Pmp* and its corresponding voltage *Vmp* and current *Imp* as explained in 4.6.5.

4.7. Model of the temperature of the PV module

In this section, the procedure followed to calculate the hourly temperature of the cells of the module is explained.

4.7.1. The effects of temperature on the I-V curve

It is important to know the temperature of the cell because it affects the whole I-V curve. When the temperature increases, the open circuit voltage decreases, the short circuit current increases slightly and the maximum power point decreases. As a consequence, at a given irradiance, if the temperature increases, the electrical efficiency of the module decreases leading to a lower power extraction. These effects are explained visually by the figure below that represents a generic module at fixed irradiance and different temperatures:

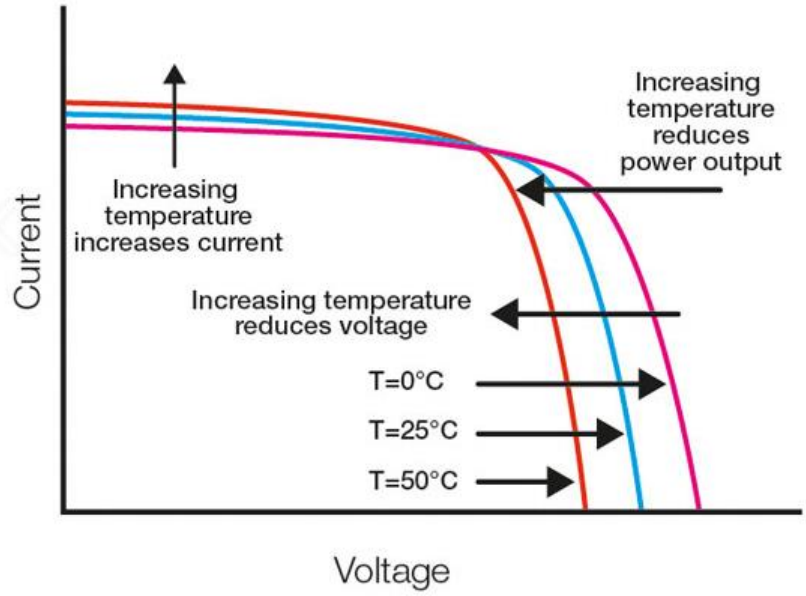

Figure 16 Effects of the temperature on the IV curve of a generic PV module. Source [13].

4.7.2. The temperature from an energy balance

To estimate the cell temperature, there are different approaches in the literature, the approach followed in this project is the one described in [4] which comes from an experimental study [20]. This approach was chosen for two main reasons. Firstly because with few parameters it provides sufficient accuracy: the temperature difference against measurements is within a range of 2°C, resulting in an error in the range of 1% in DC power against measured data by the authors [20]. Secondly because it is the one used in PVsyst [8].

The approach is based on an energy balance across the PV module, that receives heat from the irradiance of the sun and it is cooled by conduction with ambient air and by convection with the

wind. Following this reasoning, the temperature of the cell can be written as follows:

$$T_c = T_a + \frac{\alpha E_e (1 - \eta_m)}{U_0 + U_1 v_w} \tag{4.33}$$

And the efficiency of the module is given by:

$$\eta_m = \frac{P_{dc}}{E_e A_c} \tag{4.34}$$

Where: T_c is the temperature of the module (°C), T_a is the temperature of the surroundings (°C), α is the adsorption coefficient, E_e is the POA effective global irradiance on the module (W/m^2), η_m is the electrical efficiency of the module, U_0 is the constant heat transfer coefficient (W/ °C m^2), U_1 is the convective heat transfer coefficient (W/°C m^2/m/s), v_w is the wind speed (m/s), P_{dc} is the electrical power (W) and A_c is the area occupied by the cells (m^2).

The nominator of equation (4.33) represents the part of the incoming solar energy that contributes to heat up the module. This differs from the total incoming POA irradiance because part of the incoming irradiance is transformed into electricity by the photovoltaic effect (considered with the electrical efficiency η_m) and another part is reflected by the module (considered through the adsorption coefficient α). The denominator represents the overall heat transfer coefficient that the incoming power to a change in temperature.

To solve equation (4.33 for the cell temperature seven variables must be known. The hourly ambient temperature and wind speed are supposed to be known from weather data (see 4.3.1). The hourly POA effective irradiance is calculated by the program in the POA irradiance sub-model (see 4.5.8). The constant heat transfer coefficients and the adsorption coefficient are assumed with default values or known from experimental measurements as explained in section 4.7.4.The electrical efficiency of the module is calculated by the program inside the iterative loop of the temperature sub-model as explained below.

4.7.3. The algorithm used to predict the temperature

The equation (4.33 used to calculate the temperature is a function of the electrical efficiency of the module expressed by equation (4.34, the efficiency is a function of the output DC power, which in turn is a function of the temperature and irradiance (see the single diode model in Section 4.6.4). Therefore, the equation of the temperature is implicit as it is a function of the temperature itself.

Since the equation of the temperature is implicit, a numerical iterative algorithm was developed to calculate the temperature hourly: starting from an initial guess, the temperature is changed till the

difference between two steps is lower than a given tolerance. The guess value needed to start the iterative algorithm is obtained by assuming the following in equation (4.33: the temperature of the module in the first hour of the morning is equal to the ambient temperature, and then the temperature for the following hours is calculated considering the efficiency of the previous hour. This is clearly a rough approximation but is a good starting point for the algorithm: it takes at most only 3 iterations to find the temperature starting from this guess.

Once every simulation, the program performs the following steps to find the guess value:

1. The temperature of the cell at the beginning of every day is set equal to the corresponding ambient temperature

2. The temperature of the cell for all the other hours of the day is calculated considering the efficiency of previous hour in equation (4.33.

3. The old temperature is set equal to the guess temperature

For every hour, the cycle below runs till convergence is reached:

1. The new DC power is calculated with the old temperature by means of the IV model (Section 4.6.4)

2. The efficiency is calculated inserting the new DC power in equation (4.34

3. The new temperature is calculated inserting the new efficiency in equation (4.33

4. The difference between old and new temperatures is compared with the tolerance, if it is lower, the iterations are interrupted, and otherwise the cycle is repeated.

5. If the cycle continues, the old temperature is set equal to the new temperature.

This method was chosen for the sake of simplicity and to reduce computational power. Another possible way could be to write the equation of the temperature as a function of the power written explicitly in terms of I and V (both dependent on temperature) and then solve the implicit equation with a numerical solver such as e.g. Newton method. However, that was unnecessary complicated, because the proposed algorithm produces already a remarkable high level of accuracy with values varying less than 0.02 C with respect to PVsyst while keeping a moderate computational time There is clearly no reason for looking at a higher accuracy in temperature since a difference of 0.02C means an error of around 0.01-0.02% in DC power.

4.7.4. The default assumptions used in the temperature model

The parameters that need to be known or assumed for the temperature model are the heat transfer coefficients and the adsorption coefficient. Ideally, theses parameters should be calculated with

experiments. However, this is not always possible especially when comparing several different PV manufacturers. For this reason, default parameters will be used when the measured parameters are not known following the same assumptions of PVsyst. In absence of measured data, their default values are a good guideline as the authors performed several experiments with different PV panels and the simulations described well the reality as shown in the validation section of the PVsyst manual [8].

The adsorption coefficient α is set to 0.9 by default, which is a very common value used by PVsyst and others [4], [8], [20].

For the parameters *Uc* and *Uv*, the situation is more complicated. The authors of PVsyst suggest to avoid using the wind velocity if the data are not reliable and well measured. Therefore, they suggest to set *Uv* to zero. *Uc* is the only parameter used, which is the same as setting the wind speed to an average value and then summing the coefficients *U1* and *U0*. The authors of PVsyst claim that using *Uc*=29W/M2 for free standing systems, the error on the temperatures is under 1 C as shown in different conditions and experiments performed in the validation section of the PVsyst manual [8]. Since large scale PV plants have air circulating all around the panel, the default values used in this project are the ones suggested by PVsyst for free standing systems:

$$U_c = 29\ \frac{W}{m^2 K} \tag{4.35}$$

$$U_c = 0\ \frac{W}{m^2 K\ {}^{m}/_{s}} \tag{4.36}$$

Note that all the parameters can be modified in the model, but if they are not specified, the model uses the default values. An interesting further study could be the analysis of the real heat transfer coefficients from measurements as discussed in **¡Error! No se encuentra el origen de la referencia.**.

4.8. Model of the plant layout

In this section the procedure to design the layout of the plant is described. It is assumed that the desired nominal power of the plant, the PV module characteristics and the inverter characteristic are known parameters. The objective of this section is to design the total number of modules, their arrangement into strings, and the arrangement of the strings into arrays.

Note that in this project the analysis of the layout of the plant focuses only on the part of the plant from the modules to the DC/AC inverters. Everything that comes after the inverter towards the grid, such as the collection grid, the transformers and the connection point to the grid are not explicitly considered in the layout. Nevertheless, their effect is considered through coefficients that takes into account the losses in AC cables and transformers, as explained in section 4.10.2.

4.8.1. General layout of a large-scale PV plant

Generally, in large scale PV plants, the modules are gathered in arrays and for each array there is an inverter that converts the AC power coming from the array to the AC power that will be injected into the grid. Generally, there are different possible layout of the inverters:

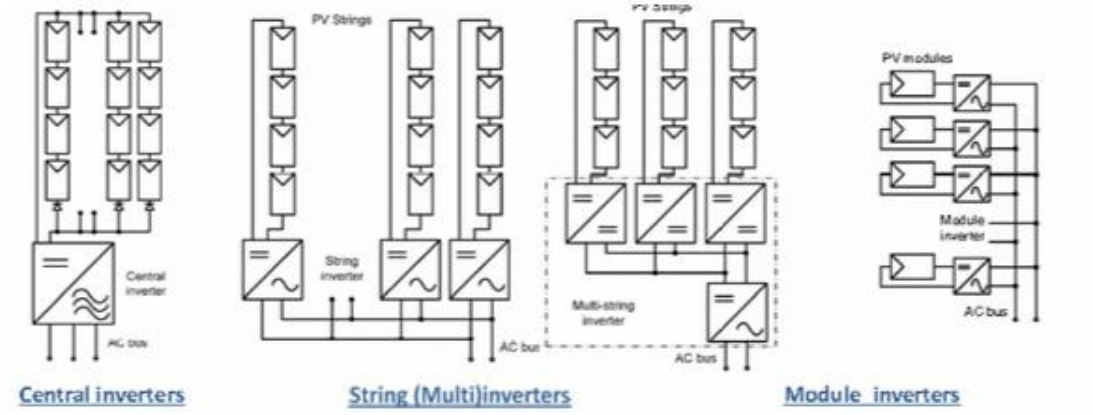

Figure 17 Schematic of the different types of inverter layouts. Source [21]

Since the present project deals with large-scale PV plants, the configuration will be of the kind of central inverter an inverter per array. The array is composed in the following way: several modules are connected in series, forming a string and different strings are connected in parallel to form an array. The figure below illustrates an example of configurations with different arrays and central inverters:

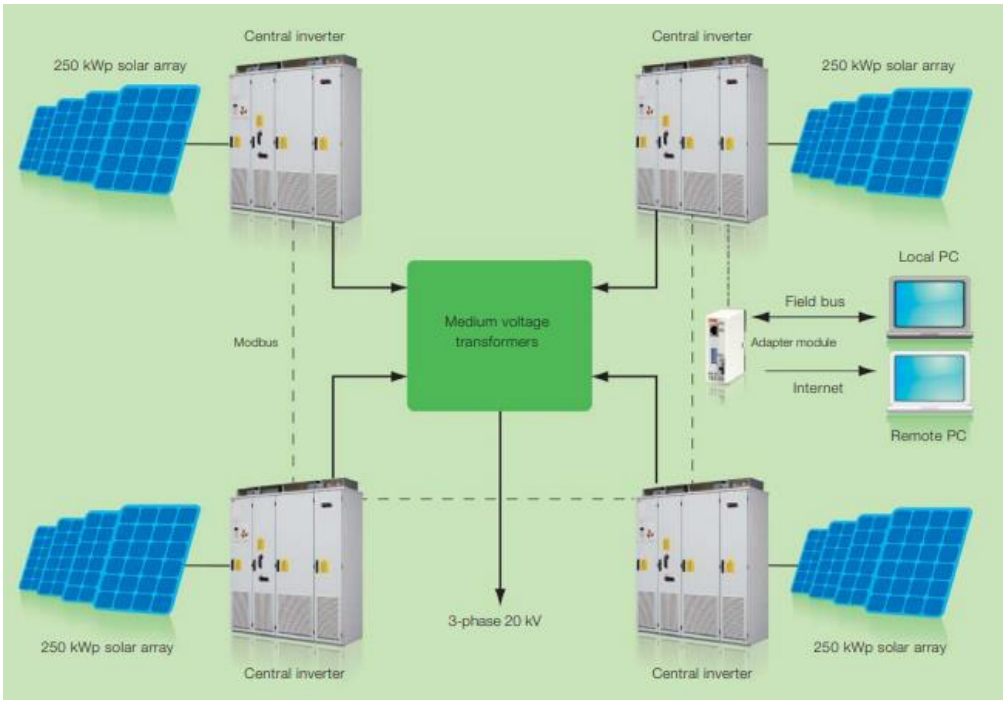

Figure 18 Schematic of a typical large-scale grid-connected PV plant. Source [22]

In the figure, each array is connected to an inverter and the AC power from few inverters is collected in a LV internal grid and then transformed to HV by step-up transformers. It should be noted that different layout options are possible for which the number of inverters per transformer changes, but this is a topic concerning the AC side of the plant which is not included in the scope of the project.

Also, it should be noted that the

4.8.2. Current and voltage in an array of modules

When connecting modules in series in one string, the current of the string is the current of the single module while the voltage of the string is the sum of the voltages of all the modules. Therefore, the number of modules in series will define the voltage of the string while the number of strings in parallel will define the current of the array, thus the power of the array as shown in the following schematic:

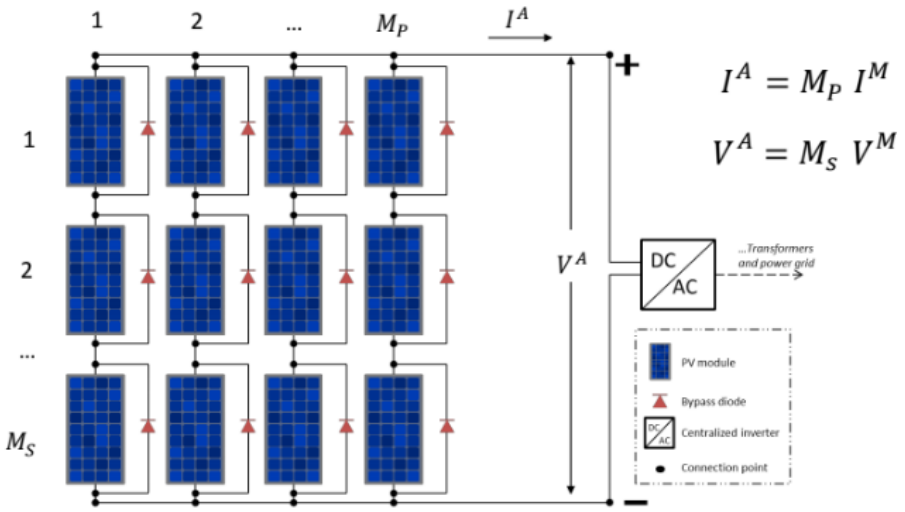

Figure 19 Schematic of a typical array layout. Source [23].

From the figure above, it is seen that the current and voltage of the array are as follows:

$$I_{array} = I_{string} \times n_{string} = I_{module} \times n_{string} \tag{4.37}$$

$$V_{array} = V_{string} = V_{module} \times n_{parallel} \tag{4.38}$$

Where n_{string} represents the number of modules in series in one string and $n_{parallel}$ represents the number of parallel strings in one array.

The total power of one array can be then easily calculated as:

$$P_{dc,array} = P_{dc,module} \times n_{parallel} \times n_{string} \tag{4.39}$$

4.8.3. Sizing the number of inverters

Deciding the number of inverters to install in a PV plant is a complex topic because it is a techno-economic decision that must take into account different diverging conditions. First of all, the power of the inverter is limited (at usually a maximum of few MW, recently ABB released a 2MW central inverter [24]) therefore for large plants many inverter must be used. Second, the inverter has a maximum power point tracking algorithm that tries to move the working point always at its maximum. When the number of modules per inverter increases, the accuracy of the MPPT decreases as the MPP of the array might not be exactly the value of MPP of each of the modules. Third, the higher the number of inverter per field, the higher the reliability of the plant, because if there is a fault on one inverter, and the field has more than one, than it can still produce power at half of the capacity instead of shutting down completely. Fourth, the increasing the number of

inverter might (or might not) increase the costs. These are among the main reasons that would pull the decisions either to increase or decrease the number of inverter. A thorough analysis that does an optimization of different techno-economic parameters, would probably require another entire project and is out of the scope of the present work.

Therefore, the strategy for the design of the number of the inverters is simplified in two steps. Firstly, the user chooses an inverter model and given a desired power the number of the inverters is calculated by:

$$n_{inverters} = n_{array} = \frac{P_{dc,field}}{P_{ac,inverter}\eta_{inv}} \tag{4.40}$$

Where $P_{dc,field}$ is the nominal DC power of the plant in W, $P_{ac,inverter}$ is the nominal AC power of the inverter and η_{inv} is the nominal efficiency of the inverter.

Secondly, the program outputs the DC-to-AC ratio calculated as:

$$DC/AC = \frac{P_{dc,array}}{P_{ac,inverter}} \tag{4.41}$$

With the DC-to-AC ratio and the clipping losses, the designer can either increase or decrease the size or number of inverters as discussed in Section 6.2 . This strategy is taken from PVsyst in which the inverter selects an inverter and a desired power and the program warns if the specific design produces high clipping losses[8].

4.8.4. Sizing the number of modules in series

To size the number of modules in a string, the limits on the voltage are applied. Since the number of modules in series will define the voltage of the string and thus the voltage of the array, this number is designed in order to respect the limits on the voltage imposed by the inverter MPPT and by the maximum voltage allowable in inverter and modules. These conditions translate into 4 inequalities as follows.

The voltage of the array must always be inside the operating range of the MPPT of the inverter:

$$V_{array,mpp,min} > V_{inv,mppt,min} \tag{4.42}$$

$$V_{array,mpp,max} < V_{inv,mppt,max} \tag{4.43}$$

The absolute maximum voltage of the array must be lower than the maximum allowable voltage of the inverter and of the module:

$$V_{array,OC,max} < V_{inv,input,max} \quad (4.44)$$

$$V_{array,OC,max} < V_{module,system,max} \quad (4.45)$$

The range for MPPT, the maximum voltage of the inverter and of the panels are known as always present in the datasheets of the components. In addition, for these four conditions, three voltages of the PV module need to be known: the maximum and minimum operating voltages and the minimum absolute open circuit voltage. By default, the program calculates them with the single diode model of the IV curve, calculating the curve at different temperatures.

It should be noted that while the single diode model is built to be precise on the maximum power point, its accuracy on the open circuit voltage should be discussed. That is why in the designing phase, to calculate the *Voc* at minimum temperature, the program allows to use the single diode model or directly the temperature coefficient of *Voc* that is usually provided by manufacturers. The choice of one or the other is left to the user of the program. The values calculated with the two methods could lead to different values and therefore to different maximum limit for the number of modules in series. This is because in the default version of the single diode model (see section 4.6.3) the value of *muVoc* is not used to build the model, therefore the *muVoc* of the model might be slightly different from the value of the manufacturers. However, this does not affect the energy yield as the power is produced at *Vmpp* and not at *Voc*. This line of reasoning and the possibility of choosing either one of the method are taken from the manual of PVsyst that discusses the topic in further details [8]. In PVsyst, the default is to calculate the maximum open circuit voltage with the single diode model, and this approach was followed in the present work.

The default design temperatures are set to the default values of PVsyst:

$$T_{max,operating} = 60\,°C \quad (4.46)$$

$$T_{min,operating} = 20\,°C \quad (4.47)$$

$$T_{min,absolute} = -10\,°C \quad (4.48)$$

Anyway, they can be changed in the parameters of the model.

Once the temperatures are defined and the way to find the desinging *Voc* is set, the software computes simultaneously all the conditions listed above and finds a range of possible numbers of modules in series.

4.8.5. Sizing the number of strings in parallel

The sizing of the number of strings per array is performed starting from the power of the strings. For each of the possible string arrangements found in section 4.8.4, the number of strings is found by respecting simultaneously the two following conditions:

$$n_{strings} = \frac{P_{array,DC}}{P_{string,DC}} \tag{4.49}$$

Or equivalently:

$$n_{strings} = \frac{n_{modules,array}}{n_{modules,string}} \tag{4.50}$$

And:

$$I_{module,max} n_{strings} \leq I_{inverter,max} \tag{4.51}$$

The first condition is needed to reach the desired power, while the second condition must be verified to comply with the technical limits of the inverter. This means that if the second condition is respected, for each of the possible number of modules in series there is a configuration with its number of strings in parallel, otherwise the configuration is not possible.

4.8.6. The possible configurations and designs of the array voltage

Once the inverter was sized, and the different configurations of number of modules in series and in parallel were calculates, a table that sums up the possible configurations and additional details (such as array voltage and current range etc.) is created:

Table 1: Typical table of possible layout configurations

Variable	***Opt.1***	***Opt.2***	***Opt.3***
N series	*15*	*16*	*17*
N parallel	*309*	*290*	*273*
Vmin	*492*	*524*	*557*
Vmax	*576*	*614*	*652*
DC Power (W)	*1483867*	*1485468*	*1485788*
AC Power (W)	*1447030*	*1448591*	*1448903*
Total modules	*4635*	*4640*	*4641*

All of the configurations generated are possible configurations that respect all the limit discussed in sections 4.8.4 and 4.8.5. However, for the final design, only one configuration must be chosen. The choice of the configuration is usually based on the voltage range of the particular configuration as this will affect the losses of the plant. The choice is not trivial because with a higher voltage, the

losses of the inverter increase while the losses of the DC cables decrease. Moreover, a third factor could be considered because the current of a string is determined by the module with the lowest current, which means that in case one of the modules in a string performs badly (because of soiling, hotspots, technical issues etc.) the current of the whole string is affected. For this last reason, a lower number of modules in string should increase the reliability of the plant. Even disregarding this last consideration, the two first conditions pulls towards two different directions therefore a tradeoff must be found. A detailed optimization is not performed in the present project and a configuration on the middle is usually chosen as default.

4.9. Model of the inverter

In this section the relationship between the inverter input power in DC and the inverter output AC power is presented. In the present project the inverter is considered as a black box and the it models only the transfer function between the inputs and the output, which is the efficiency which is the same as in PVsyst and in SAM. The algorithm to model the inverter is taken from SAM, because an explicit algorithm from PVsyst could not be found.

4.9.1. The Sandia inverter model with empirical coefficients

The algorithm proposed by SAM [9] is based on a study in which the behavior of the inverter is modelled through four experimental parameters [25]. The relationship between DC power and AC power reads as follows:

$$P_{ac} = \left[\frac{P_{ac,0}}{A-B} - C(A-B)\right](P_{dc}-B) + C(P_{dc}-B)^2 \tag{4.52}$$

Where:

$$A = P_{dc}\left[1 + C_1(V_{dc} - V_{dc,0})\right] \tag{4.53}$$

$$B = P_{so}\left[1 + C_2(V_{dc} - V_{dc,0})\right] \tag{4.54}$$

$$C = C_0\left[1 + C_3(V_{dc} - V_{dc,0})\right] \tag{4.55}$$

Where the variables are: *Pac* is the AC power output of the inverter, *Pdc* is the DC power input of the inverter, *Vdc* is the DC voltage input of the inverter

The physical parameters of the inverter, usually available in datasheets, are:

1. Pac,0= the rated AC power of the inverter
2. Pdc,0= the rated DC power input at the inverter to reach the rated AC power output
3. Vdc,0=the rated DC voltage input at the inverter at which the rated powers are calculated
4. Ps0=the minimum DC power input to start the inversion process, usually called inverter self-consumption (by SAM) or power threshold (by PVsyst).
5. Pnt=AC power needed by the inverter during the night

The experimental C coefficients used to build the model are:

1. C0=empirical coefficient that introduce the quadratic relationship between DC power in and the AC power out at the reference voltage Vdc,0.
2. C1, C2, C3 are three empirical coefficients that make the parameters Pdc,0 Pso, and C0 vary linearly with the voltage.

An explanatory figure from the study on which this model is based [25] shows the relationship between DC power and AC power for three different voltages, the rated quantities and the curvature are shown:

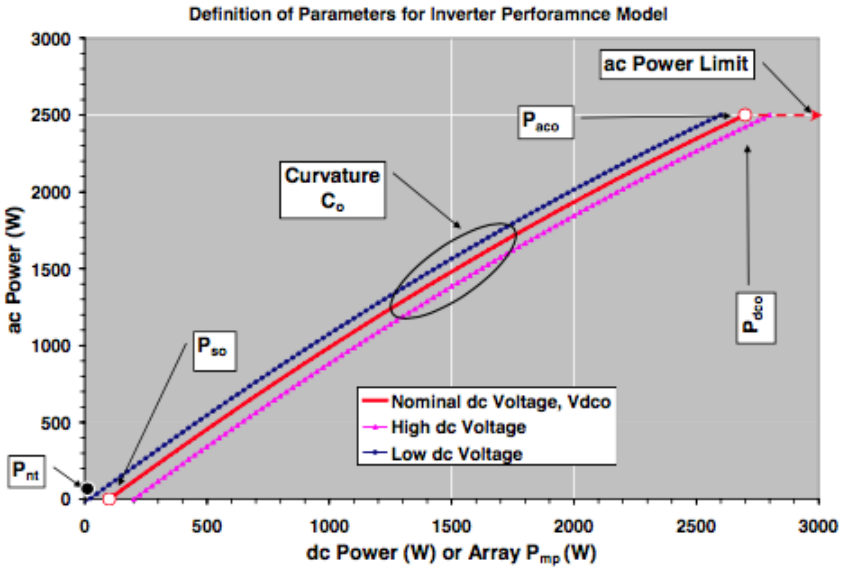

Figure 20 AC power versus DC power for three DC voltage levels according to the Sandia inverter performance model. Source [25].

As it can be seen by the figure above, the relationship between Pac and Pdc is almost linear. However, in reality it is slightly quadratic with respect to the power at a given voltage. Moreover, the power threshold, the inverter operating consumption and the parameter C0 expressing the quadratic relationship between Pdc and Pac vary with the voltage. Therefore, the relationship is finally a nonlinear function of both power and voltage that can be generally expressed as:

$$P_{ac,out} = f(P_{dc,in}, V_{dc,in}) \tag{4.56}$$

It should be noted that if the equation (4.52 is written as a function of input voltage and power, the resulting polynomial would contain several terms and the relationship with both V and P together would be higher than quadratic (there would be terms as high as V^3,PV^2,P^2V etc). Still, at a given voltage, all the empirical C coefficients are constant, A, B and C are constants and the AC power out is a quadratic function of the DC power. By substituting the constants with the generic letter *k*, and rewriting the equation (4.52), the quadratic relationship is clearly visible:

$$P_{ac,out} = K_1(P_{dc} - K_2) + K_3(P_{dc} - K_4)^2 \tag{4.57}$$

4.9.2. The Sandia inverter model with only the inverter datasheet

This model is supposed to be used with the C coefficients calculated from experimental measurements. These parameters can be found for example in the database of the software SAM, and come from tests performed on each model. If the inverter used can be found in a database, all the above mentioned parameters of the inverter datasheet and the empirical C coefficients are supposed to be available. Therefore, all the coefficients A, B and C of the above equation can be calculated and the model is completed. However, if the inverter is not in the database, as it happens frequently, the model was developed to work only with the data from the manufacturer datasheet. As explained in [25], if no values for the C coefficients are available, the C coefficients are all set to zero by default. The relationship between DC power in and AC power out becomes:

$$P_{ac} = \left[\frac{P_{ac,0}}{P_{dc,0} - P_{s,0}}\right](P_{dc} - P_{so,0}) \tag{4.58}$$

The above equation shows that the relationship between *Pdc* in and *Pac* out is now linear and there is no dependency on the voltage any more. In facts, by setting *C0*=0, the quadratic relationship becomes linear and by setting the other *C* coefficients to zero, the dependency on the voltage is eliminated.

Since the above equation relies only on data from the datasheets, which does not usually provide all of them, some assumptions on the parameters are made following the reasoning explained in the SAM reference manual [9] based on a previous study [25]:

Pdc,0 is the DC input power at which the rated AC power is obtained, and it is usually not available, therefore it is calculated with the rated efficiency: Pdc,0=Pac,0/eta, 0 . However, a proper definition of “rated efficiency” has not be found in the source [25], where it is said to use either the peak

efficiency or the CEC/EU efficiency. Therefore, the CEC or EU efficiency will be used in the present work, and if not available, the maximum efficiency will be used instead. The weighted efficiency is chosen as the first choice because PV inverter usually do not reach their maximum efficiency at rated power, but instead at lower power as explained in the note at the end of the section.

Pso,0 is the DC input power needed to start the conversion (also called inverter self-consumption) and if not available from the inverter datasheet, it is assumed to be 1% of the rated DC power Pdc,0 as advised in [25].

Pac0 is the rated AC power of the inverter, which is always available.

It should be noted that the setting C0=0 in the above equation, the relationship between Pdc in and Pac out becomes linear, and if the efficiency is calculated as Pacout/ Pdcin:

$$\eta_{inv} = \frac{P_{ac,0}}{P_{dc,0} - P_{s,0}}\left(1 - \frac{P_{s,0}}{P_{dc}}\right) \tag{4.59}$$

It can be noted that the efficiency increases when Pdc in increases, which means that at maximum power in there is the maximum of the efficiency. However, as already said above, this is usually not the case for PV inverters where the maximum is somewhere around 60% of the rated dc power as suggested by PVsyst [8] or 50% as suggested by the authors of a study that compares different modelling approaches [26]. This paper suggested that even without the empirical coefficients, the value of C0 should be set to a default so that the quadratic behavior is preserved. The authors suggest that the default value of C0 could be taken assuming that the known maximum efficiency occurs when Pdc,in =50%. Even though this approach might increase the accuracy, in the present work it has not been applied, because it was preferred to follow the original Sandia model, which does not include it.

4.9.3. Night consumption and power clipping

The SANDIA inverter model applies the following limits to the power input and output:

At night, when clearly Pdc=0, the inverter power output Pac=-Pnight, because the inverter needs power to stay on and sense if some power from the PV panels is received. However, in the present model, this option can be deactivated and night consumption set to zero, because theoretically the inverter could be switched off during nighttime, and switched on before the sun rises.

During the day, if Pdc<Pso then the inverter power Pac=-Pnight. This check is always activated because during the day the inverter is effectively always on.

During the day if Pdc>Pdc,0 then the inverter output power is set to Pac= Pac,0. The inverter clips the power in excess by changing the operating point of the I-V curve away from its maximum. The clipped power is stored in a vector as it might be needed for analysis, for example in the study case

presented in this project the financial loss related to the clipped (and therefore wasted) power was analyzed against the gain in reducing the inverter size as explained in section 6.

It should be noted that when the input power is higher than the rated power of the inverter, the inverter is not overloaded because it is supposed that the mppt algorithm changes the operating point away from the maximum and therefore the panels will produce less power. The figure below from the manual of PVsyst (which makes the same assumption) illustrate how the operating point is shifted:

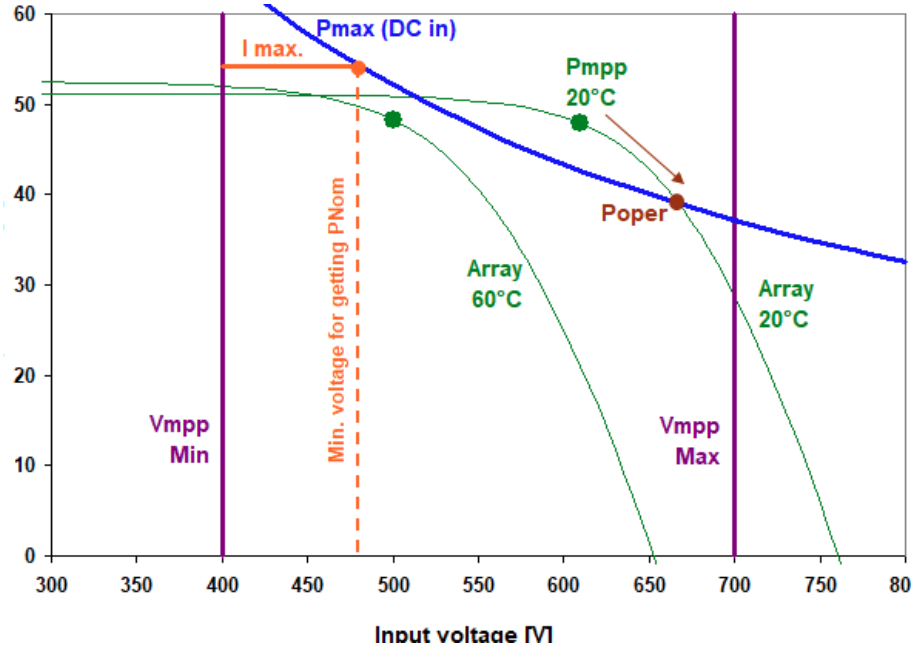

Figure 21 Schematic of the shift of working point in a typical clipping mechanism of an inverter. Source [8]

In the case illustrated above, the operating point of the inverter was moved towards a higher voltage, thus allowing the inverter to receive its maximum rated power without running the risk of overloading it.

4.9.4. The model of the inverter with defined efficiency

If the efficiency of the inverter is available for different operating powers, and for different operating voltages, the efficiency at any operating power and voltage is calculated as a linear interpolation between the known values in two steps: the interpolation must be done for the power and for the voltages because the efficiency is dependent on both variable.

A similar reasoning is followed by PVsyst that allows to define the efficiency for 9 different power ratio and 3 different voltages [8]. This method will be more precise if the data are available. However, this kind of data is difficult to obtain and the SANDIA inverter model is used as a default.

4.10. Model of the losses of the plant

This section introduces the losses of the plant that have not explicitly been considered in other sections. These losses are the DC cable losses and the AC cable and transformer losses. Optical losses are treated in section 4.5, effects of the temperature are treated in section 4.7, and inverter losses are treated in section 4.9.

4.10.1. DC cabling losses

To calculate the DC cabling losses, in theory a detailed analysis with sizing of the different sections of the cables is needed. However, in the present project, a simpler approach is used that allows to consider a first approximation of the DC losses of the plants without having to perform a detailed design of the cables. This approach is taken from the first approximation approach used by PVsyst in treating DC losses. PVsyst also offers a specific tool to effectively model the cable losses in a precise way. However, this second approach has not been implemented in the present project for the sake of simplicity, but could certainly be an interesting further development.

The first approximation used by PVsyst calculates the DC losses is performed by setting a specific resistance of the wire as a percentage of the standard resistance of the array, in three steps. Firstly, the standard resistance of the array is calculated as voltage over current of the array. Secondly, the resistance of the wires is set to a percentage of the standard resistance of the array. Thirdly, the ohmic losses of the cables are calculated with the resistance of the wires and the current of the array. The three steps can be summarized as:

Calculated once per simulation:

$$R_{array} = \frac{V_{array,STC}}{I_{array,STC}} \tag{4.60}$$

$$R_{dc,wiring} = R_{array} P_{loss,STC} \tag{4.61}$$

Calculated every hour:

$$P_{loss,dc,cables} = R_{dc,wiring} I_{array}^2 \tag{4.62}$$

With the above equation, it is possible to calculate a first approximation of the DC losses of the plant by only using one parameter. The percentage of $R_{dc,wiring}$ with respect to R_{array} is set to 1.5% by default following the default value of PVsyst. This parameter can anyway be modified at any simulation.

Although this approach is a first approximation, it is nevertheless already an improvement with

respect to models that calculate only a yearly percentage loss. Because it allows the loss to vary with the current, therefore for example it can be an indicator to choose the specific configuration of the layout of the plant as described in 4.8.6.

It should be noted that to avoid large amount of losses in the DC cables transporting power to the main AC inverters, it is usually good practice to put many panels in series so that the voltage is increased while the current is kept at the value of one single module. While lowering the DC losses, this method could lead to high mismatch losses because the current is limited by the lowest current in a string, and if one panel in a string is performing badly, it will affect all the others [4].

4.10.2. AC cabling and transformer losses

The AC cable losses and the transformer losses are considered only through a yearly percentage loss factor. This is the default method used in SAM (also for DC cables). PVsyst instead offers a more detailed approach in which the cables and transformers are modeled. However, this last approach has not been followed for the sake of simplicity, but could be an interesting further development. In the present model, the losses are expressed as:

$$\eta_{ac,cables} = 1 - L_{ac,cables} \tag{4.63}$$

$$\eta_{ac,transformer} = 1 - L_{ac,transformer} \tag{4.64}$$

The default values of losses are both set to 1% and can be modified at any moment.

4.11. Model of the energy yield

This section introduces the procedure followed to calculate the hourly and yearly energy injected to the grid. It supposes that the energy output from the arrays is already computed hourly (see section 4.8.2). Since in the program the time step at which power is calculated is one hour, and the energy is expressed as kWh, the value of energy and power are the same at a given hour.

The power flow can be summarized in five steps. First, the global horizontal irradiance arriving from the sun is adjusted to calculate the effective POA irradiance that hits the cells, introducing losses related to the tilt of the panel and optical losses. Second, the energy arriving from the sun is transformed by the modules in electric energy trough the photovoltaic effect which is modeled by the single diode model (see section 4.6). Third, the DC energy is collected at each array with DC cables that introduce ohmic losses (see section 4.10.1). Fourth, the DC power coming from the arrays is converted to AC power by the inverters, introducing the inverter losses modeled in section 4.9. Fifth, the AC power output from the inverter is transported to the point of connection to the grid passing through AC cables and step up transformers, introducing losses described in 4.10.2. Finally, the energy yield injected to the grid can be calculated as:

$$E_{grid,hourly} = \sum_{i=1}^{n\_inverter} (E_{ac,inv,out,i}) \, \eta_{ac,cables} \, \eta_{ac,transformer} \tag{4.65}$$

Where: $\eta_{ac,transformer}$ and $\eta_{ac,cables}$ cables are the efficiencies of transformers and AC cables (see section 4.10.2).

The software calculates all the variables hourly, and by simply summing all the values over one year, the yearly energy output can be computed as:

$$E_{grid,yearly} = \sum_{1}^{8760} E_{grid,hourly} \, F_{availaibility} \tag{4.66}$$

Availability is an additional optional parameter that is used to take into account that the plant might be unavailable during certain hours of the year, as done by SAM [9].

4.12. Model of the LCOE

When assessing costs and the economic feasibility of a technology in electrical power generation, one of the most important indicator is the levelized cost of electricity (LCOE). The LCOE is a way to express what is the cost of producing one unit of energy (Kwh) with a particular technology. It calculates all the costs needed during the lifetime of the project and divide them by the total amount of energy that the project is expected to produce. The LCOE can also be thought as the minimum price at which electricity should be sold to reach the desired return on investment. The LCOE is a very important indicator as it can be used to compare different technologies with different lifetime, different fuels, different energy production, different costs etc.

The formula used in this project to calculate the LCOE is taken from the methodology of the International Renewable Energy Agency (IRENA) [27] :

$$LCOE = \frac{\sum_{t=1}^{n} \frac{I_t + M_t + F_t}{(1+r)^t}}{\sum_{t=1}^{n} \frac{E_t}{(1+r)^t}} \tag{4.67}$$

Where: I_t represents all the investments in year t, M_t represents all the operations and maintenance expenditures (O&M) in the year t, F_t represents all the fuel expenditures in year t, E_t is the electricity generation in year t, r is the discount rate and n is the life of the system.

The nominator is the present value of all costs of the plants during its lifetime and the denominator is the present value of all the electricity produced over the lifetime of the project.

In this project the generalized form can be further simplified with the following assumptions:

1. The sun is free: there are no fuel expenditures
2. The investments are considered to be performed at year 0, beginning of the project: CAPEX is out of the sum in the nominator.
3. The discount rate is the weighted average cost of capital or WACC (see below)
4. The yearly production is affected by the degradation of the panels, and it can be expressed as linear degradation or percentage decrease (D).
5. The residual value of the system is considered to be zero.

Therefore the formula can be re-written as the typical formula used in the solar industry [28]:

$$LCOE = \frac{CAPEX + \sum_{t=1}^{n} \frac{OPEX}{(1+WACC)^t}}{\sum_{t=1}^{n} \frac{Y_0(1-D)^n}{(1+WACC)^t}} \quad (4.68)$$

The CAPEX represent all the investments that were made at the beginning of the project such as costs of the modules, inverters, cabling etc. (a detailed cost breakdown is presented in section 6.3.2.1). The OPEX represents all the yearly costs needed for the operation and maintenance of the plant.

The discount rate that is usually used when analyzing renewable energy projects is the weighted average cost of capital: it is a weighted average of the expected rate of return of the various investors. RES projects frequently involve financing from equity and debt. There might be different equity/debt ratio and the different parties could have different expectations for the return on investment. Therefore, the WACC weights differently the discounts rates of the two parties. WACC is given by::

$$WACC = Eq_{\%} IRR_{\%} + Debt_{\%} i_{debt}(1 - T_{corp}) \quad (4.69)$$

Where: $Eq_{\%}$ is the percentage of CAPEX that is equity, $IRR_{\%}$ is the expected Internal rate of return of the equity financiers or cost of equity, $Debt_{\%}$ is the percentage of CAPEX that is debt, i_{debt} is the interest rate of the debt, or expected Internal rate of return of the debt financiers or cost of debt and T_{corp} is the corporate tax rate.

Note that the corporate tax rate is included in the formula because the annual interest on a debt is tax deductible. This is among the reasons why debt financing is an interesting option for large projects: if the cost of equity and debt are the same, it could be more convenient to increase the debt percentage. In facts, thanks to tax deductions, a higher debt percentage would overall reduce the WACC.

In this project the LCOE was calculated with the formula expressed above as it is the general simplified formula that agencies like IRENA use [27].

More complex approaches can be used, such as the one used by Lazard [29] in which the all the financials variables are calculated separately for each year, and the LCOE is found as the selling price of electricity that allows to obtain the desired IRR. However, the simplified approach used in this project is detailed enough as the value of WACC can be found in literature and the results can be easily compared with the ones of most of the agencies using the same approach (such as IRENA, etc).

Since LCOE can be though as of the minimum price at which electricity should be sold to reach the desired WACC, the higher the WACC the higher the LCOE. Moreover, the WACC is country dependent, and can change case by case [30].

5. Validation of the models

In this section the validation of the model developed is described in two parts: first, each sub model is tested separately with the same input of the sub model and then an overall validation of the whole model is presented. Usually, when validating a model, the results of a simulation are compared with measured data to see the accuracy of the prediction of the model. However, in the present project the validation is performed against result coming from PVsyst or eventually from SAM, because the technical equipment to test real scenarios was not available and accurate measurements would have required measurements of parameters for a long time (even several years) which could have not been done.

Since PVsyst was used as a reference and it is trusted by the industry as discussed in Section 4.1 results of the present project are considered satisfactory if they get close to the ones of PVsyst. PVsyst, was developed during years and several validations of this software are available, for example from [8].

To perform the validation, the hourly values of the output file from the code written in the present project and the output file from the advanced simulation done in PVsyst are compared.

5.1. Validation of the complete model

During the development of this model, a validation was performed for each sub-model, both software run with exactly the same inputs, and the outputs are compared, so that the results were not affected by discrepancies in the inputs (that might come from a previous model). However, in a real simulation, the inputs of the model are introduced only once, and each sub model has as inputs the outputs of the previous sub model which already contain an error, therefore the overall error will be amplified. In this section the whole simulation is tested starting from the same weather file, module and inverter. Clearly, in PVsyst and in the software developed all the parameters that should be assumed are set at the same values (e.g. the heat transfer coefficient, the albedo etc.).

The following table summarizes the results of the validation, performed with the 1 MW plant using the same inverter and module of the case study (Section 6.3.1) a with a weather file synthetically generated in Barcelona (the accuracy of the file is not important as it will just serve as the input for both software).

Table 2 Validation RMSE and MBD for four main variables

Sub-Model	RMSE	MBD	Reference Model
Global Effective	0.15%	0.046%	PVsyst
Cell Temp. Heat transfer	0. 08%	0.022%	PVsyst
DC power	0.27%	0.074%	PVsyst

As it can be seen from both the table the RMSE for DC power is 0.27%, and since the accuracy of PVsyst is around 1% if compared with measured data, it is considered a very positive and satisfactory result, because it means that given a weather file, both models will predict the hourly energy output with an error below 1%.

6. Case Study: the effect of under sizing the inverter

In this section, a case study on the economic effects of under sizing the inverter on the LCOE and CAPEX of the plant is presented.

6.1. Case study objective

The study case analyses the effects of under-sizing the inverter on the LCOE of the plant. When designing a PV power plant, it is important to know the DC nominal power of the solar field and to carefully select the AC rated power of the inverters. Since solar panels produce the nameplate power only under standard conditions of G=1000W and T=25 degrees, and these conditions happen only few times during the year, the solar field will almost always produce less than its nominal capacity, therefore the inverter could be smaller than the solar field. The ratio of the DC power of the solar array to the AC power of the inverter is called DC-to-AC ratio. The relationship between the LCOE of the plant and the DC-to-AC ratio will be studied in the next sections with the objective of finding the DC-to-AC ratio that minimizes the LCOE.

The problem is known to the solar industry, and different studies were performed on the topic from different points of view, such as [31] that analyses the financial effects or [32] that analyses the impact on the reliability of the inverter. Many deal with the financial effects of under sizing the inverter but generally the conclusions are drawn always for generic location. The purpose of this case study is instead to quantitatively relate the quality of the irradiance to the best DC-to-AC ratio. As a result, just only analyzing the weather file, one could be able to have a general guideline on the size of the inverter.

This case study is an interesting application where the software developed in the present project is particularly useful. The software has a specific model for the technical performance and the LCOE model, and can run in loops by changing the sizing parameters at every simulation. Therefore, it can output results for different locations with different sizing with just one run. Moreover, the ability of the software to work with hourly variables is crucial as the study of energy losses due to clipping and energy gains due to higher efficiency of the inverter would not be possible without hourly values.

6.2. Case study methodology

In different locations the effect of changing the DC-to-AC ratio was studied. The variables analyzed are LCOE, the CAPEX and the capacity factor of the plant. For all the simulations, the model of the inverter, the module and all the modelling parameters and the financial assumptions are the same.

For each location, the study was performed in four step. First, a weather file was selected for the particular location. Second, the technical simulation runs for different DC-to-AC ratios and outputs

yearly energy yield and clipping losses from hourly values. A matrix of DC-to-AC ratios, corresponding capacity factor and clipping losses is obtained. Third, the model LCOE model runs with the above mentioned matrix, adding two columns of corresponding LCOE and total CAPEX. Fourth, the DC-to-AC ratio at which the LCOE reaches the minimum is found.

It should be noted that the DC-to-AC ratio can vary in two ways: by under-sizing the inverter or oversizing the solar field. The latter was preferred for two reasons. First because the DC power of the solar field can be easily increased by simply increasing the number of strings in parallel, which does not imply changing the module and does not change the array voltage, but only the current. Since the array voltage is a design parameter needed to choose an inverter, if the array voltage stays the same the inverter can be the same, thus having the same design. On the other hand, if given a fixed solar field, the inverter size is changed, it implies changing the inverter model every time the DC-to-AC ratio changes, which complicates the simulation and introduces inconsistencies in the analysis (because the results could be affected by a different intrinsic efficiency of a different inverter model etc.)

6.3. Case study assumptions

6.3.1. Technical assumptions

This analysis is a general analysis that has the objective of providing results regardless of the specific inverter or module installed. However, for the program to run, a specific model of both components must be chosen, therefore components from world top manufacturers are chosen as described below.

6.3.1.1. Module

The module chosen is JinkoSolar 320PP-72 for the following reasons. First, The manufacturer Jinkosolar was chosen as it is one of the world top PV manufacturers and it is considered tier 1 by Bloomberg [33]. Second, the model 320PP-72 was chosen as it was suggested in the conference Solar Parity held in Milan, June 2018. The parameters used for the single diode model described in Section 4.6.2 are taken from the database of PVsyst 6.3.

6.3.1.2. Inverter

The inverter chosen is ABB PVS800-57 1000KW for the following reasons. First, ABB is one of the world top for solar inverters. Second, the model PVS800 was chosen because is among the most installed ABB PV central inverter (globally over 6.5GW installed) and it is based on R8i which is the most used inverter module in the world (globally over 100GW installed) [34].The power of 1000KW has been selected because the nominal power of the plant is 10MW, which means that 10 central inverters should be installed and this is aligned with the designing strategy discussed in 4.8.3. The parameters used for the simulation are taken from PVsyst database, with the definition of the

efficiency in different points and voltages as discussed in section 4.9.4. For more details, the complete inverter datasheet is present in the annexes.

6.3.1.3. Model parameters

For the simulations, all the model parameters are set to the default values because a generic plant is considered. All the assumptions are described in the section of each sub-model and the following table summarizes the value given to each of the variable:

Table 3 Technical parameters for the analysis on under-sizing the inverter

Variable	*Value*	*Unit*	*Sub-model*	*Section*
DHI/GHI	from data	-	Erb's correlation	4.3.2
Albedo	0.2	-	POA ground diffuse	4.5.3
b	0.05	-	Beam IAM	4.5.5
IAMs	from table	-	Sky IAM	4.5.6
IAMg	from table	-	Ground IAM	4.5.6
SF	1	-	Effective Irradiance	4.5.7
Alfa	0.9	-	Temperature	4.7.2
U0	29	$\mathrm{W/m^2K}$	Temperature	4.7.2
U1	0	$\mathrm{W/m^2K/m/s}$	Temperature	4.7.2
Tmax	60	$\mathrm{°C}$	Sizing voltage	4.83
Tmin	20	$\mathrm{°C}$	Sizing voltage	4.84
Tmin abs	-10	$\mathrm{°C}$	Sizing voltage	4.85
PlossSTD	1.5%	-	Ohmic losses	4.10.1
Lac cables	1%	-	AC cabling losses	4.10.2
Lac trans	1%	-	Transformer losses	4.10.2
Favailability	1	-	Energy yield	4.11

6.3.2. Financial Assumptions

In this section, the financial assumption used to estimate all the economic parameters of the LCOE formula (see Section 4.12) are presented.

6.3.2.1. CAPEX Assumptions

PV plants require a large initial investment and then can run for their entire lifetime with no costs for fuel and limited O&M, therefore CAPEX is the most significant source of costs when assessing

a PV project. Different sources were analyzed to obtain the CAPEX for the PV plant [1], [35], [36]. These sources present different costs, but this is reasonable as the costs are quite dependent on the region:

Table 4 CAPEX breakdown by different sources

Source	*[1]*	*[35]*	*[36]*
CAPEX modules (eur/kWh)	483	530	375
CAPEX inverter (eur/kWh)	115	110	84
CAPEX BoS (eur/kWh)	552	335	280
CAPEX total	**1150**	**975**	**739**

The data from an European study which provides a cost breakdown for PV plants in Germany [35] were used because this European study provides a detailed cost breakdown for PV plants in Germany [35] which is fundamental to understand how much of the cost is related to the AC side of the plant. The table below shows the cost breakdown:

BoS component	€/kWp 2014	Area-related share 2014	€/kWp area-related 2014	€/kWp area-related reduction by 2030	Other reduction by 2030	€/kWp other reduction by 2030
Inverter	110	0 %	0	0	Learning curve	
Mounting structure	75	100 %	75	23	16 %	12
Installation work	50	100 %	50	15	11 %	6
DC cables	50	75 %	38	11	9 %	4
Grid connection	60	0 %	0	0	24 %	15
Infrastructure	40	75 %	30	9	9 %	4
Planning & docum.	35	75 %	26	8	7 %	2
Transformer	20	0 %	0	0	13 %	3
Switch gear	5	0 %	0	0	11 %	1
Total BoS	**445**	**49 %**	**219**	**66**	**10 %**	**45**

Figure 22 CAPEX breakdown for large scale PV plants. Source [35].

These data were modified to obtain the cost breakdown divided in the 3 needed sections: Modules, AC dependent and other costs.

The cost of a plant can be thought of being dependent on:

1. The DC side of the plant, or the number of the solar modules (e.g. solar modules, the

mounting structures, DC cables, etc.)

2. The AC side of the plant (inverters, transformers, grid connection etc.)

3. Fixed costs (planning, documentation, etc.)

The source provided an estimate of the proportion of the cost that was area dependent. The area is clearly mainly dependent on the number of PV modules, therefore the dependency on the area can be seen as more or less dependency of the Kwdc of the plant. To work out the costs related to the AC side of the plant, all the costs related to the area were excluded and the following assumptions were used to take into account that some of the non-area dependent costs could be fixed costs, therefore not dependent on the AC side either:

1. The costs related to the AC side are the costs of: inverter, grid connection, infrastructure, transformers and switchgears only.

2. The cost of inverters, grid connection and transformers are 100% proportional to the KWac.

3. The cost of the Infrastructure is 15% proportional to the AC side

This is summarized in the following table:

	Eur/Kw	**Area Dependency**	**AC Dependency**	**AC Corrected**	**Eur/kw AC-Dependent**	**% on Total**
Inverter	110	0%	100%	100%	110	12%
Mounting	75	100%	0%	0%	0	8%
Installation	50	100%	0%	0%	0	5%
DC cables	50	75%	25%	0%	0	5%
GRid Connection	60	0%	100%	100%	60	6%
Infrastructure	40	75%	25%	15%	6	4%
Planning and Docum	35	75%	25%	0%	0	4%
Transformer	20	0%	100%	100%	20	2%
Switch Gear	5	0%	100%	50%	2.5	1%
Module	500	100%	0%	0%	500	53%

The final percentages were multiplied by the total CAPEX available from the CAPEX of the second column of table Table 4 from source [35] that was finally used to obtain a cost breakdown in the 3 parts, as summarized in the table below:

Table 5 CAPEX breakdown divided by the AC and DC side

Source	*[35]*
CAPEX DC side (eur/kWh)	530
CAPEX AC side (eur/kWh)	255
CAPEX Other (eur/kWh)	335
CAPEX total	**975**

6.3.2.2. OPEX Assumption

All the sources cited above were consulted to find the value of the OPEX, which was finally taken as 15 eur/Kw/year from [35] for consistency with the CAPEX assumptions (that were taken from the same source).

6.3.2.3. WACC Assumptions

As previously said, the WACC have a big impact on the total costs of the plant and on the LCOE. When WACC increases the cost of capital increases. In other words, it means that for the same plant, with a higher WACC, a higher part of the revenues goes to investors or as interests thus increasing the overall cost of the plant. The following graph clearly shows this concept:

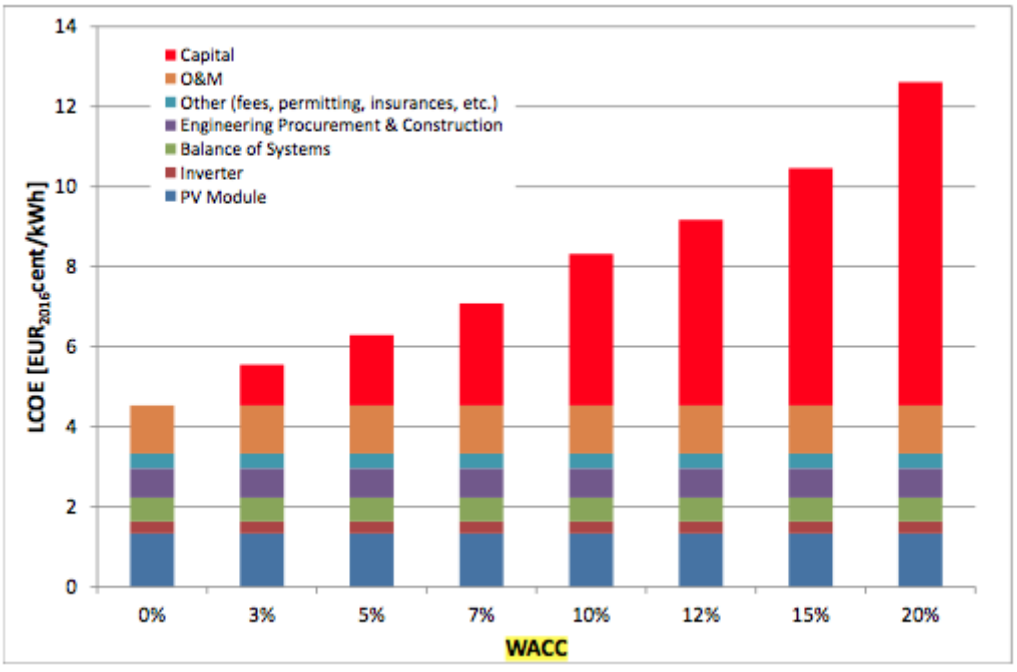

Figure 23 LCOE for PV systems as a function of the WACC. Source [37]

As can be seen, higher WACC means higher cost of capital, while all the other costs are constant.

It is remarkable to see that at WACC=10% the cost of capital is roughly 50% of the total cost. According to the literature, the WACC can be very different in different countries, the following map shows average WACC values in Europe:

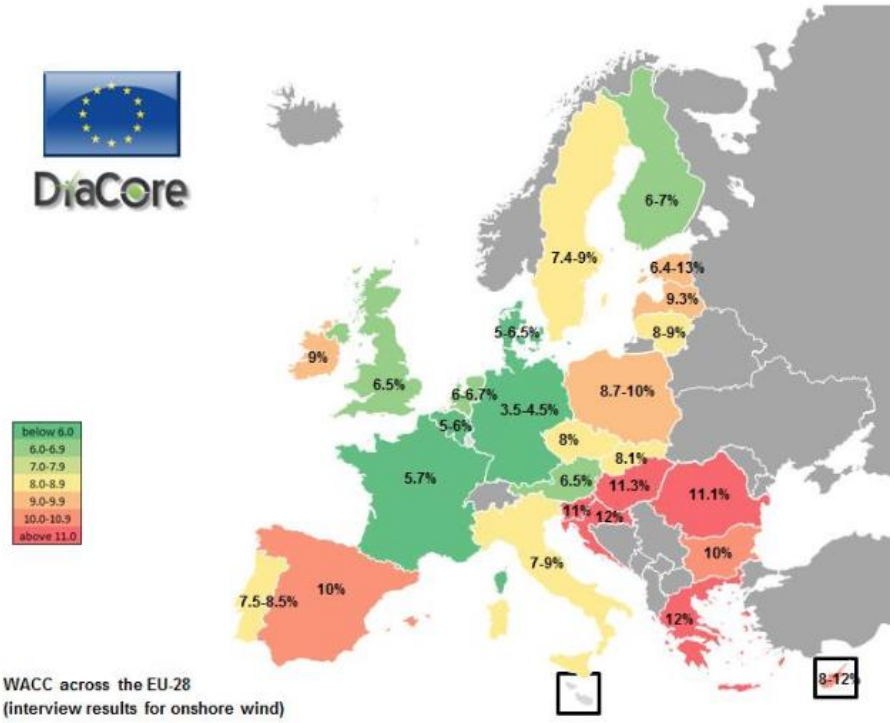

Figure 24 Map of suggested WACC in wind energy projects for different countries in Europe. Source [38]

Even though it is for onshore wind, the source states that for large PV plants in Spain, WACC is likely to be higher than 10% [30]. Another source mentions values around 7.5 % on a survey done in Spain [38]. The agency IRENA uses 7.5% for its calculations [1] and another source creates scenarios from 2% to 10% [5]. Therefore, in the present project values of 7% was used.

6.4. Case study plant layout

In this section the plant layout obtained by setting the software with the parameters listed in 6.3.1 is presented. After running the simulation, the results of the plant layout with DC-to-AC ratio = 1.25 can be summarized by the following table:

Table 6 Layout results of the 10MW solar PV plant base case

Variable	***Value***
Field Nominal power	10MW
Narray	8
Nseries	19
Nparallel	205
Array total modules	3895
Field total modules	31160
ArrayVmin	780
ArrayVmax	900
Array DC power (STC)	9971

For each of the 8 arrays, the I-V curve is:

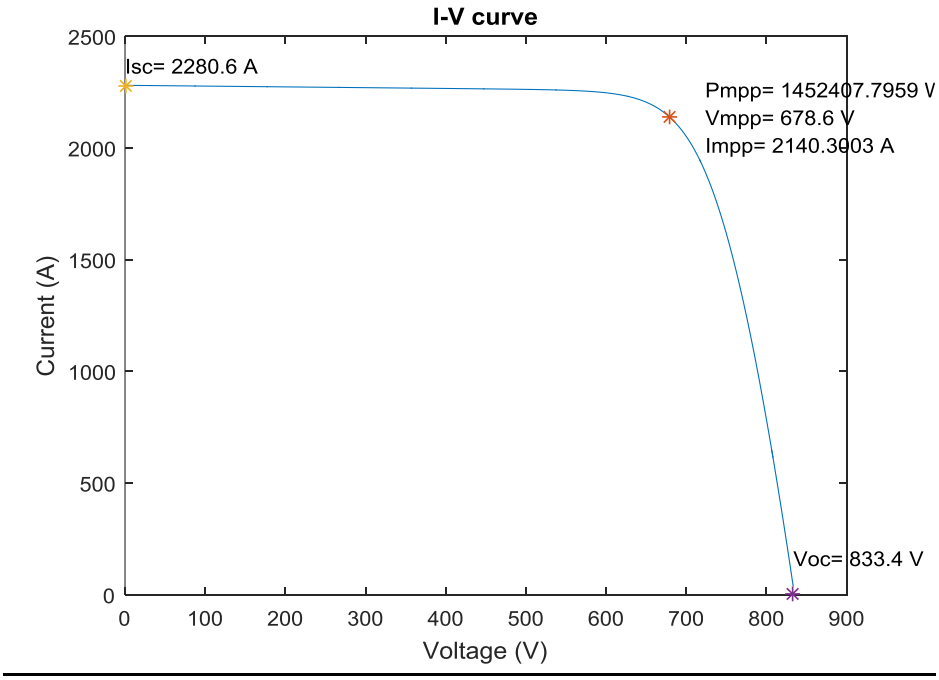

Figure 25 Typical I-V curve of any of the array in the case study

6.5. Case study results

In this section the results of the case study are analyzed, first, a general view on one particular location is presented, and then results of different locations are summarized in a table and the

relationship between the DC-to-AC ratio and the mean irradiance is shown.

The graphs below show how LCOE and CF change varying the DC-to-AC ratio for the simulation performed in Barcelona, and London:

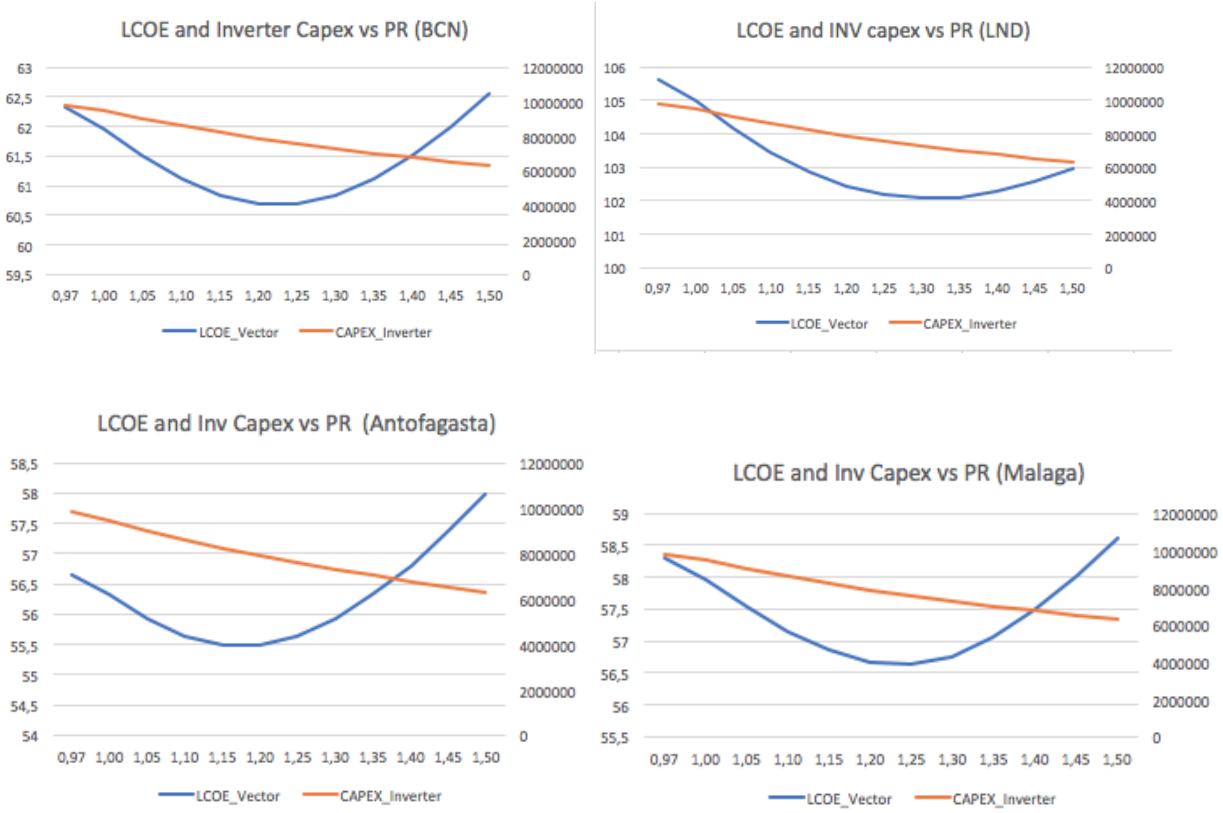

Figure 26 Results of the analysis: LCOE (eur/kwh) and CAPEX versus power ratio in Barcelona, London, Antofagasta and Malaga

The CAPEX of the plant decreases proportionally with the DC-to-AC ratio because the CAPEX of the AC side of the plant is assumed to be proportional to the installed AC power which decreases when increasing the DC-to-AC ratio, at a given installed DC power.

The LCOE decreases, reaches a minimum and increases again due to the combined effects of CF and CAPEX. Before the minimum, for low DC-to-AC ratios, it decreases because the gains in reduced CAPEX outweigh the slight decrease in CF. The opposite happens after the minimum, leading to an increase in LCOE. The values of LCOE of around 60eur/kWh for example Barcelona are compatible with values of Madrid with the same WACC=7% presented in Figure 4 thus meaning that the parameters of the analysis lead to reasonable results.

If the capacity factor is analyzed, for example for London, which is quite an extreme case as it is affected by low mean irradiance, the results would be as follows:

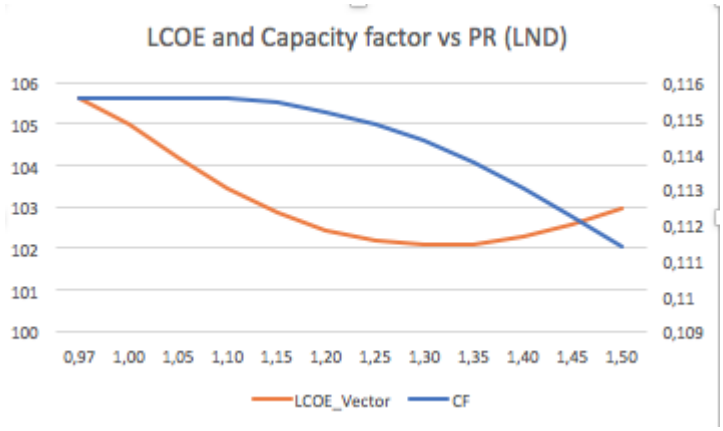

Figure 27 LOCE (eur/kwh) and capacity factor as a function of the Power ratio

As it can be seen, the capacity factor has an initial plateau, or a slight increase and then drops. This is because for low DC-to-AC ratios the clipping losses are zero or very low, and the inverter will work most of the time on the part of the inverter efficiency curve for which the efficiency is higher. Further increasing the DC-to-AC ratio results in higher clipping losses that outweigh the gains in efficiency and lead to a decrease in capacity factor.

In other words, the minimum corresponds to a tradeoff between savings on a smaller inverter and losses due to clipping. For this reason, the optimal solution would be to design the plant with the DC-TO-AC ratio corresponding to the minimum LCOE, from now on referred to as the suggested DC-to-AC ratio.

Different locations were tested, and as expected the minimum of LCOE is reached for different DC-to-AC ratio, due to the different irradiance in the different locations. For example, in places where the irradiance is higher like Málaga and Antofagasta where the DC-to-AC ratio is lower, while in London it is much higher. The results of the simulations for different locations are summarized in the table below:

Table 7 Summarized results of the analysis with optimal DC-to-AC ratio for different locations

	Antofagasta	*Malaga*	*Barcelona*	*Stockholm*	*London*
Average Irradiance (KWh/M2)	1992	1829	1630	975	975
Capacity Factor	0.215	0.209	0.194	0.120	0.114
Optimal DC-to-AC ratio	1.15	1.2-1.22	1.21-1.24	1.25-1.3	1.3-1.35

As it can be seen, locations with a better irradiance reach the minimum LCOE for lower values of the DC-to-AC ratio. This is due to the fact that if the irradiance is better it is more likely that the plant outputs power close to the DC nominal condition, which is higher than the AC maximum power and

therefore the excess power is clipped. etc.

It is interesting the case of London and Stockholm have the same average yearly irradiance, while different capacity factor. The reason behind it is that in London the lower frequency at which STD conditions are reached means that most of the time the system will output DC power much lower than the nominal DC power, and this is the reason why a higher DC-to-AC ratio is suggested. On the other hand, in Stockholm the frequency of STD conditions is higher, and the system is more likely to output DC power closer to the DC nominal power, thus increasing the clipping losses if the inverter is too small, therefore a lower DC-to-AC ratio is suggested.

6.6. Case study conclusions

The case study proved that it makes financial sense to oversize the solar field with respect to the inverter. The values of LCOE of around 60eur/kWh for example Barcelona are compatible with values of Madrid with the same WACC=7% presented in Figure 4 thus meaning that the parameters of the analysis lead to reasonable results. Reduction in the investment of the inverter is around 15-35%, which in turns decreases the total CAPEX by 3-5%. The reduction in total capex is of course lower as the AC side of the plant accounts for roundabout 20% of the investment. Reduction in LCOE due to optimal Dc-to-AC ratio ranges between 3.3%-3.7% depending on the location.

It should be noted that the case study did not take into account the possible consequences of under-sizing the inverter on the reliability and maintenance costs of the inverter itself. This is linked to the behavior of the components inside the inverter, which is another interesting study case studied for example in [32] but out of the scope of this project. As a future work, it would be interesting to combine both aspects together to obtain a more comprehensive result.

7. Planning, costs and environmental impact of this project

7.1. Environmental Impact of the project

D

As with the economics, the environmental impact of a solar PV plant will be calculated for the 10MW plant described in section 6.4. The environmental impact due to greenhouse gases (GHG) emissions is treated in the following sections.

7.1.1. Emissions of a solar PV plant with life cycle assessment

To calculate the environmental impact of an electricity generation technology, it is usual practice to consider the life cycle assessment (LCA). The LCA takes into account all the emissions of a technology, dividing the lifecycle of a plant in three phases: upstream process (manufacturing, plant construction etc.), operational process (power generation, fuel needed, O&M, etc.) and downstream process (power plant decommissioning, disposal etc.) as shown by the figure below:

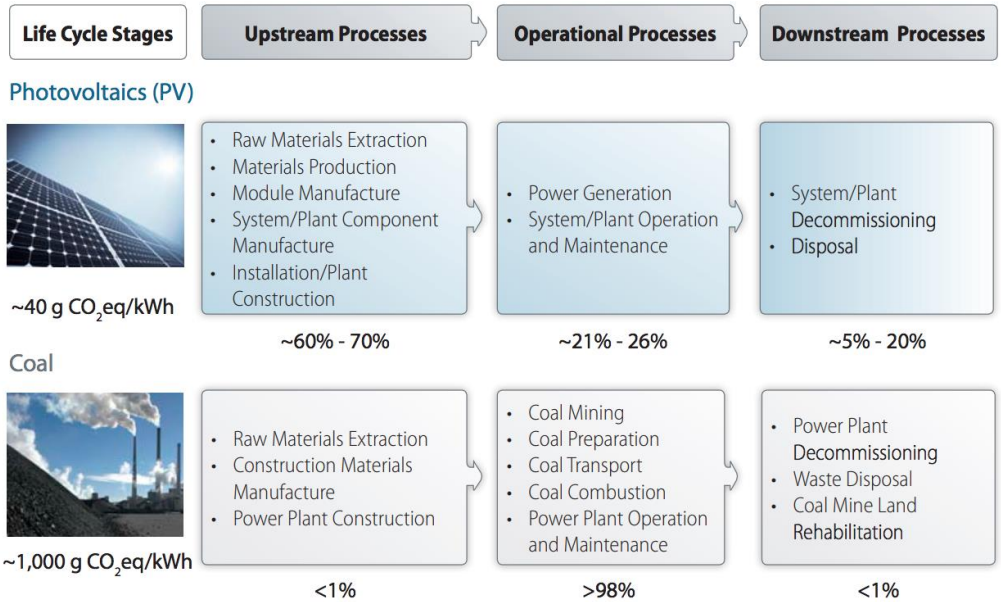

Source: *Burkhardt et al. (2012) and Whitaker et al. (2012) Photos from iStock/19291390 and iStock/1627655, Top (left to right): Photo from iStock/13737597, NREL/PIX 18553, iStock/12123595, NREL/PIX 16933, NREL/PIX 18968, NREL/PIX 19163*

Figure 28 The three stages of the lifecycle of PV and Coal plant. Source NREL [39].

Calculating a LCA in details is a complex topic that alone require another study and is often subjected to discrepancies. Therefore, for the analysis of this section, the data obtained from a study by NREL will be used [39]. The analysts reviewed more than 400 studies and considering a lifetime of 30 years, they finally conclude that the LCA greenhouse gases emissions of crystalline

silicon solar PV system is around 40 g CO2eq/kWh. This value is very low if compared for example with coal, for which LCA emissions are estimated at 1000 g CO2eq/kWh, it is instead slightly higher than other RES as shown in the figure below from the same study:

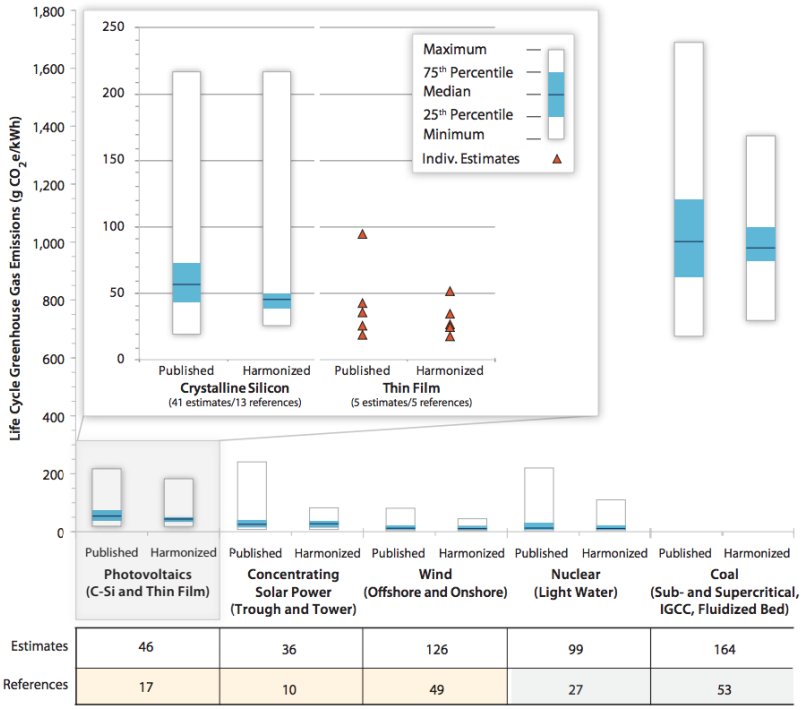

Figure 29 Life Cycle Greenhouse Gases Emissions for different RES and coal. Source NREL [39].

7.1.2. Avoided Emissions

While GHG emissions of PV plants are not the lowest among renewable technologies, it is sure that the emissions of a PV plant are always lower than any of the fossil-fueled plants. Since almost any country has a large amount of electricity produced with fossil fuels, when producing electricity with PV, the net result is that some emissions are avoided, because the electricity would otherwise be produce with higher emitting plants.

For example, consider a case in which the electricity produced with the 10 MW solar plant would be otherwise produced with a coal plant. Recalling that they emit respectively 40 g CO2eq/kWh and 1000 g CO2eq/kWh, the avoided emissions thanks to the installation of the solar PV plant will be:

$$\text{Avoided } CO_2 \text{ Emissions} = (1000 - 40) \times 10000 \times 8760 \times 30 \times 0.19 = 489440\text{t} \qquad (7.1)$$

This means that when a 10MWPV plant is installed in place of a coal plant, the avoided emissions are equal to 489,440 tons of CO2eq. Now, obviously the energy mix of a country is composed by several different technologies which have emit differently. Therefore, an average of the emissions weighted on the proportion of the specific technology in the energy mix is usually defined as the

grid emission factor. Taking the case of Spain, the grid emission factor was considered to be 343 g CO2eq/kWh in 2013, calculated with the LCA method in a study by the European Union [40]. In this case, the avoided emissions thanks to the installation of the 10MW solar PV plants will be:

$$\text{Avoided } CO_2 \text{ Emissions} = (343 - 40) \times 10000 \times 8760 \times 30 \times 0.19 = 151290\text{t} \qquad (7.2)$$

Still, installing a 10MWPV plant in same would save the emissions of 151,290 tons of CO2eq. This reasoning could be repeated for any other country and there will be always some avoided emissions, unless the country has an emission factor lower than 40 g CO2eq/kWh, which is not the case in any of the European countries [40]. Therefore, installing solar PV panels, is always a solution that reduces the GHG emissions, even considering the manufacturing and the disposal of the panels.

8. Conclusions

Results of the program against results from PVsyst showed that the hourly RMSE for the DC power is 0.26%, leading to the conclusion that the program developed in the present project simulates well the parameters of a PV plant and it is a good starting point for a possible further development.

The case study proved that it makes financial sense to oversize the solar field with respect to the inverter. The values of LCOE of around 60eur/kWh for example Barcelona are compatible with values of Madrid with the same WACC=7% presented in Figure 4 thus meaning that the parameters of the analysis lead to reasonable results. Reduction in the investment of the inverter is around 15-35%, which in turns decreases the total CAPEX by 3-5%. The reduction in total capex is of course lower as the AC side of the plant accounts for roundabout 20% of the investment. Reduction in LCOE due to optimal Dc-to-AC ratio ranges between 3.3%-3.7% depending on the location.

This project was developed from zero, therefore the scope has to be limited to the models described in Section4.2. Nevertheless, it was precisely the of the project to develop a software that could be further developed by other students or researchers. During the developing of the software, interesting topics were encountered that could be further studied, as an example:

1. A detailed model of the control scheme of the plant or integrating this model to other models to analyze different issues related to PV (such as the integration to the grid etc.)
2. A model to retrieve the model parameters of the I-V curve of the single diode model from experimental measurements done at different T and G.
3. A model to consider the self-shading losses due to adjacent rows.
4. A study on the techno-economic strategy to design the optimum number of inverters given a plant size.
5. A study that considers the effects of under-sizing the inverter on the reliability of the inverter itself

This is a list of possible problems that were encountered and could not be analyzed due to time restrictions, but could certainly be extended by others.

Bibliography

[1] IRENA, “Renewable Power Generation Costs in 2017,” 2018.

[2] IEA, “Photovoltaic Power Systems Programme - PVPS Annual Report 2016,” *Int. Energy Agency*, p. 130, 2016.

[3] European Commision Energy Roadmap 2050, “Communication from the Commission to the European Parliament, the Council, the European Economic and Social Committee and the Committee of the Regions, COM/2011/0885 final.,” 2011.

[4] P. Altermatt, *Photovoltaic Solar Energy: From Fundamentals to Applications*. 2017.

[5] E. Vartiainen *et al.*, “The True Competitiveness of Solar PV - A European Case Study,” 2017.

[6] J. A. Duffie and W. A. Bekman, *Solar Engineering of Thermal Processes*. Wiley, 2013.

[7] K. J. Sauer and T. Roessler, “Systematic approaches to ensure correct representation of measured multi-irradiance module performance in PV system energy production forecasting software programs,” *IEEE J. Photovoltaics*, vol. 3, no. 1, pp. 422–428, 2013.

[8] A. Mermoud, “PVsyst 6 Help,” *PVsyst SA*, 2018. [Online]. Available: http://files.pvsyst.com/help/. [Accessed: 01-Apr-2018].

[9] P. Gilman, A. Dobos, N. DiOrio, J. Freeman, S. Janzou, and D. Ryberg, “SAM Photovoltaic Model Technical Reference SAM Photovoltaic Model Technical Reference,” 2018.

[10] B. Y. H. Liu and R. C. Jordan, “The interrelationship and characteristic distribution of direct, diffuse and total solar radiation,” *Sol. Energy*, vol. 4, no. 3, pp. 1–19, Jul. 1960.

[11] R. R. Perez, P. Ineichen, E. L. Maxwell, R. D. Seals, and A. Zelenka, “Dynamic global-to-direct irradiance conversion models,” in *ASHRAE Transactions*, 1992.

[12] College of Engineering and Applied Science University of Colorado Boulder, “Solar Angles and Tracking Systems - Lesson - TeachEngineering,” *Integrated Teaching and Learning Program*. [Online]. Available: https://www.teachengineering.org/lessons/view/cub_pveff_lesson01. [Accessed: 20-Jul-2018].

[13] Seaward Group USA, “Frequently asked questions about Curve Tracing.” [Online]. Available: http://www.seaward-groupusa.com/userfiles/curve-tracing.php. [Accessed: 20-Jul-2018].

[14] T. Maor and J. Appelbaum, “View factors of photovoltaic collector systems,” *Sol. Energy*, vol. 86, no. 6, pp. 1701–1708, 2012.

[15] PVsyst SA, “PVsyst Photovoltaic Software 6.7.3.” 2018.

[16] N. Pearsall, *The performance of photovoltaic (PV) systems : modelling, measurement and assessment*. Woodhead Publishing, 2017.

[17] K. J. Sauer, T. Roessler, and C. W. Hansen, “Modeling the irradiance and temperature dependence of photovoltaic modules in PVsyst,” *IEEE J. Photovoltaics*, vol. 5, no. 1, pp.

152–158, 2015.

[18] A. Mermoud and T. Lejeune, “Performance Assessment of a Simulation Model for Pv Modules of Any Available Technology,” *25th Eur. PV Sol. Energy Conf.*, no. September, pp. 6–10, 2010.

[19] A. Quarteroni and F. Saleri, *Calcolo scientifico: Esercizi e problemi risolti con MATLAB e Octave*. 2008.

[20] D. Faiman, “Assessing the outdoor operating temperature of photovoltaic modules,” *Prog. Photovoltaics Res. Appl.*, vol. 16, no. 4, pp. 307–315, 2008.

[21] UPC, “Photovoltaic Solar Energy- Course at UPC.” 2017.

[22] ABB, “ABB central inverters PVS800 100 to 500 kW - Datasheet,” p. 6, 2013.

[23] KTH, “Renewable Energy Technology 2 - Course at KTH.” 2016.

[24] ABB, “ABB central inverter, PVS800, now available up to 2 MW size,” 2017. [Online]. Available: http://www.abb.com/cawp/seitp202/c7e6d5056e761ac5c1258163003d3612.aspx. [Accessed: 20-Jul-2018].

[25] D. L. King, S. Gonzalez, G. M. Galbraith, and W. E. Boyson, “Performance Model for Grid-Connected Photovoltaic Inverters,” Albuquerque, New Mexico 87185 and Livermore, California 94550, 2007.

[26] A. Driesse, P. Jain, and S. Harrison, “Beyond the curves: Modeling the electrical efficiency of photovoltaic inverters,” in *Conference Record of the IEEE Photovoltaic Specialists Conference*, 2008.

[27] IRENA, “RESOURCE Your Source for Renewable Energy - Data Methodology,” 2015. [Online]. Available: http://dashboard.irena.org/download/Methodology.pdf. [Accessed: 01-Jul-2018].

[28] C. Tjengdrawira, M. Richter, and I. T. Theologitis, “Best Practice Guidelines for PV Cost Calculation,” 2016.

[29] LAZARD, “Lazard’s Levelized Cost of Energy Analysis - Version 11.0,” 2017.

[30] P. Noothout, D. de Jager, and et al., “The impact of risks in renewable energy investments and the role of smart policies,” 2016.

[31] K. Zipp, “Why array oversizing makes financial sense,” *Solar Power World*, p. 5, 2018.

[32] A. Sangwongwanich, Y. Yang, D. Sera, F. Blaabjerg, and D. Zhou, “On the Impacts of PV Array Sizing on the Inverter Reliability and Lifetime,” *IEEE Trans. Ind. Appl.*, vol. 54, no. 4, pp. 3656–3667, 2018.

[33] Jinko Solar, “Jinko Solar | Your Best Supplier of Modules,Cells & Wafers,” 2018. [Online]. Available: https://www.jinkosolar.com/about_207.html. [Accessed: 20-Jul-2018].

[34] T. Toissalo, “Aurinkoinverttereitä maailmalle-Aurinkoinen pientuotanto -ABB seminaari,” 2017.

[35] E. Vartiainen, G. Masson, and C. Breyer, “PV LCOE In Europe 2014-30 - Final Report,” 2015.

[36] Spain’s Photovoltaic Union - UNEF and International Energy Agency - IEA, “National Survey Report of PV Power Applications in Spain,” 2015.

[37] A. Jäger-waldau, *PV Status Report 2016*, no. October. 2016.

[38] Grant Thornton, “Renewable energy discount rate survey results – 2017,” 2018.

[39] NREL, “Life Cycle Greenhouse Gas Emissions from Solar Photovoltaics,” p. 2, 2012.

[40] B. Koffi, A. Cerutti, M. Duerr, A. Iancu, A. Kona, and G. Janssens-Maenhout, “CoM Default Emission Factors for the Member States of the European Union Dataset -Version 2017, European Commission, Joint Research Centre (JRC),” 2017.